

# Living Polymerization of 1-Hexene by Cationic Zirconium and Hafnium Complexes that Contain a Diamido/Donor Ligand of the Type $[\text{H}_3\text{CC}(\text{2-C}_5\text{H}_4\text{N})(\text{CH}_2\text{Nmesityl})_2]^{2-}$ . A Comparison of Methyl and Isobutyl Initiators

Parisa Mehrkhodavandi, Richard R. Schrock,\* and Lara L. Pryor

Department of Chemistry, Massachusetts Institute of Technology, 77 Massachusetts Avenue, Cambridge, Massachusetts 02139

Received June 5, 2003

Addition of  $[\text{Ph}_3\text{C}][\text{B}(\text{C}_6\text{F}_5)_4]$  to  $[\text{MesNpy}]\text{Hf}(\text{i-Bu})_2$  (**1a**;  $[\text{MesNpy}]^{2-} = [\text{H}_3\text{CC}(\text{2-C}_5\text{H}_4\text{N})(\text{CH}_2\text{N-2,4,6-Me}_3\text{C}_6\text{H}_2)_2]^{2-}$ ) yields  $\{[\text{MesNpy}]\text{Hf}(\text{i-Bu})\}[\text{B}(\text{C}_6\text{F}_5)_4]$  (**2a**) quantitatively. Compound **2a** decomposes in a first-order manner at 0 °C in  $\text{C}_6\text{D}_5\text{Br}$  with  $k_d = 9.2 \times 10^{-6} \text{ s}^{-1}$ . The polymerization of 1-hexene by **2a** at 0 °C in  $\text{C}_6\text{D}_5\text{Br}$  was found to follow first-order kinetics with a  $k_p = 0.10(1) \text{ M}^{-1} \text{ s}^{-1}$ . The polymerization is well-behaved up to 10 °C with  $\Delta H^\ddagger = 10.82 \text{ kcal mol}^{-1}$  and  $\Delta S^\ddagger = -23.01 \text{ cal mol}^{-1} \text{ K}^{-1}$  (at  $[\text{Hf}] = 1 \text{ M}$ ). Up to 600 equiv of 1-hexene were polymerized by **2a** in chlorobenzene to give atactic poly[1-hexene] with the expected  $M_n$  values and polydispersities between 1.02 and 1.05. Compound **1a** could be activated with  $\text{B}(\text{C}_6\text{F}_5)_3$  to yield  $\{[\text{MesNpy}]\text{Hf}(\text{CH}_2\text{CHMe}_2)\}[\text{HB}(\text{C}_6\text{F}_5)_3]$  (**2a'**), which will polymerize 1-hexene in  $\text{C}_6\text{D}_5\text{Br}$  at 0 °C with  $k_p = 0.048(1) \text{ M}^{-1} \text{ s}^{-1}$  and in toluene with  $k_p = 0.0111(3) \text{ M}^{-1} \text{ s}^{-1}$ . Well-behaved inhibitors for 1-hexene polymerization include diisopropyl ether, hexyltrimethylsilyl ether, triethylamine, and tributylamine, but not diphenyl ether or dimethylaniline, both of which undergo CH activation. Activation of  $[\text{MesNpy}]\text{Zr}(\text{i-Bu})_2$  (**1b**) with  $[\text{Ph}_3\text{C}][\text{B}(\text{C}_6\text{F}_5)_4]$  in  $\text{C}_6\text{D}_5\text{Br}$  gave  $\{[\text{MesNpy}]\text{Zr}(\text{i-Bu})\}[\text{B}(\text{C}_6\text{F}_5)_4]$  (**2b**), which decomposed at 0 °C by  $\beta$ -hydride elimination in a first-order manner with  $k_d = 8.3 \times 10^{-6} \text{ s}^{-1}$ . Polymerization of 100 equiv of 1-hexene by **2b** appeared to be well-behaved at temperatures up to 10 °C ( $\Delta H^\ddagger = 8.08 \text{ kcal mol}^{-1}$  and  $\Delta S^\ddagger = -33.34 \text{ cal mol}^{-1} \text{ K}^{-1}$  for  $[\text{Zr}] = 1 \text{ M}$ ), although sensitivity of **1b** to light limited reproducibility in general. Activation of  $[\text{MesNpy}]\text{ZrMe}_2$  (**4**) with  $[\text{Ph}_3\text{C}][\text{B}(\text{C}_6\text{F}_5)_4]$  resulted in formation of primarily catalytically inactive  $\{[\text{MesNpy}]_2\text{Zr}_2\text{Me}_3\}[\text{B}(\text{C}_6\text{F}_5)_4]$ . However,  $\sim 10\%$  of the theoretical amount of  $\{[\text{MesNpy}]\text{ZrMe}\}[\text{B}(\text{C}_6\text{F}_5)_4]$  is not trapped by  $[\text{MesNpy}]\text{ZrMe}_2$  and therefore is available to initiate polymerization of 1-hexene slowly at room temperature. Bulk polymerization results obtained for this system support the assertion that only  $\sim 10\%$  of the added metal centers are active for polymerization. Activation of  $[\text{MesNpy}]\text{HfMe}_2$  with  $[\text{Ph}_3\text{C}][\text{B}(\text{C}_6\text{F}_5)_4]$  also results in formation of inactive  $\{[\text{MesNpy}]_2\text{Hf}_2\text{Me}_3\}[\text{B}(\text{C}_6\text{F}_5)_4]$ .

## Introduction

The living Ziegler–Natta polymerization of  $\alpha$ -olefins has been a topic of interest for a number of years.<sup>1</sup> However, progress in the area took a leap forward in 1996 with McConville's report of a diamido titanium system that carried out living 1-hexene polymerization (in neat 1-hexene) at room temperature.<sup>2,3</sup> (This catalyst turned out not to be stable at low olefin concentration.<sup>4</sup>) In the past several years several groups, including ours, have reported nonmetallocene group IV catalysts<sup>5–7</sup> that

carry out what appear to be living  $\alpha$ -olefin polymerizations for various olefins under certain conditions.<sup>8–22</sup>

(1) Coates, G. W.; Hustad, P. D.; Reinartz, S. *Angew. Chem., Int. Ed.* **2002**, *41*, 2236.

(2) Scollard, J. D.; McConville, D. H. *J. Am. Chem. Soc.* **1996**, *118*, 10008.

(3) Scollard, J. D.; McConville, D. H.; Vittal, J. J.; Payne, N. C. *J. Mol. Catal. A Chem.* **1998**, *128*, 201.

(4) Scollard, J. D.; McConville, D. H.; Rettig, S. J. *Organometallics* **1997**, *16*, 1810.

(5) Kempe, R. *Angew. Chem., Int. Ed.* **2000**, *39*, 468.

(6) Britovsek, G. J. P.; Gibson, V. C.; Wass, D. F. *Angew. Chem., Int. Ed.* **1999**, *38*, 428.

(7) Gade, L. H. *Chem. Commun.* **2000**, 173.

(8) Baumann, R.; Davis, W. M.; Schrock, R. R. *J. Am. Chem. Soc.* **1997**, *119*, 3830.

(9) Schrock, R. R.; Bonitatebus, P. J., Jr.; Schrodi, Y. *Organometallics* **2001**, *20*, 1056.

(10) Jayaratne, K. C.; Sita, L. R. *J. Am. Chem. Soc.* **2000**, *122*, 958.

(11) Jayaratne, K. C.; Keaton, R. J.; Henningsen, D. A.; Sita, L. R. *J. Am. Chem. Soc.* **2000**, *122*, 10490.

(12) Keaton, R. J.; Jayaratne, K. C.; Henningsen, D. A.; Koterwas, L. A.; Sita, L. R. *J. Am. Chem. Soc.* **2001**, *123*, 6197.

(13) Tshuva, E. Y.; Goldberg, I.; Kol, M. *J. Am. Chem. Soc.* **2000**, *122*, 10706.

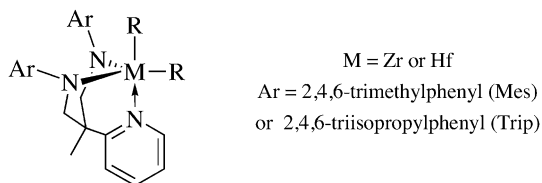
(14) Tshuva, E. Y.; Goldberg, I.; Kol, M.; Goldschmidt, Z. *Chem. Commun.* **2001**, 2120.

(15) Tshuva, E. Y.; Groysman, S.; Goldberg, I.; Kol, M.; Goldschmidt, Z. *Organometallics* **2002**, *2002*, 662.

(16) Tian, J.; Hustad, P. D.; Coates, G. W. *J. Am. Chem. Soc.* **2001**, *123*, 5134.

(17) Keaton, R. J.; Jayaratne, K. C.; Fettinger, J. C.; Sita, L. R. *J. Am. Chem. Soc.* **2000**, *122*, 12909.

We have been interested primarily in multidentate diamido ligands that contain a donor between the two amido groups, so-called diamido/donor ligands. Most recently we have focused on zirconium and hafnium complexes that contain the  $[\text{H}_3\text{CC}(2\text{-C}_5\text{H}_4\text{N})(\text{CH}_2\text{N-Mes})_2]^{2-}$  ( $[\text{MesNpy}]^{2-}$ ) ligand.<sup>23–25</sup> The trimethylsilyl-substituted version of this ligand was reported by Gade,<sup>7,26,27</sup> who has explored its coordination chemistry extensively in recent years. Our belief that trimethylsilyl substituents on nitrogen are not likely to be as stable in a cationic group 4 metal complex as aryl or *tert*-butyl substituents<sup>28</sup> led us to prepare the mesityl-substituted versions,  $\text{H}_2[\text{MesNpy}]$ . We have reported the synthesis of zirconium and hafnium dialkyl complexes that contain  $[\text{ArNpy}]^{2-}$  ligands (Ar = mesityl or 2,4,6-triisopropylphenyl).<sup>25</sup> These dialkyl species are stable when M = Hf even when R = *i*-Pr, *n*-Bu, or *i*-Bu. We also have reported in a preliminary fashion the activation of zirconium dimethyl and diisobutyl complexes in bromobenzene-*d*<sub>5</sub> with  $[\text{Ph}_3\text{C}][\text{B}(\text{C}_6\text{F}_5)_4]$  to give cationic species that are active for the polymerization of 1-hexene.<sup>23</sup>



The  $\{[\text{MesNpy}]\text{Zr}(\text{i-Bu})\}[\text{B}(\text{C}_6\text{F}_5)_4]$  catalyst formed by activation of the diisobutyl species consumed 100 equiv of 1-hexene between  $-20$  and  $10$  °C in a smooth and well-behaved reaction that was first-order in 1-hexene. On the other hand, activation of  $[\text{MesNpy}]\text{ZrMe}_2$  with  $[\text{Ph}_3\text{C}][\text{B}(\text{C}_6\text{F}_5)_4]$  produced a catalyst that would polymerize 1-hexene only very slowly, even at room temperature, as a consequence of formation of largely inactive  $\{[\text{MesNpy}]_2\text{Zr}_2\text{Me}_3\}[\text{B}(\text{C}_6\text{F}_5)_4]$ . Activation of  $[\text{MesNpy}]\text{Hf}(\text{i-Bu})_2$  in  $\text{C}_6\text{D}_5\text{Br}$  with 1 equiv of  $[\text{Ph}_3\text{C}][\text{B}(\text{C}_6\text{F}_5)_4]$  at  $-20$  °C led to formation of a  $\{[\text{MesNpy}]\text{Hf}(\text{i-Bu})\}[\text{B}(\text{C}_6\text{F}_5)_4]$  species that appeared to be more stable than the zirconium analogue.<sup>24</sup> Consumption of 1-hexene by  $\{[\text{MesNpy}]\text{Hf}(\text{i-Bu})\}[\text{B}(\text{C}_6\text{F}_5)_4]$  in  $\text{C}_6\text{D}_5\text{Br}$  at  $0$  °C followed first-order kinetics, and the resulting polymer (1-hexene) (containing up to 600 equiv of 1-hexene) was

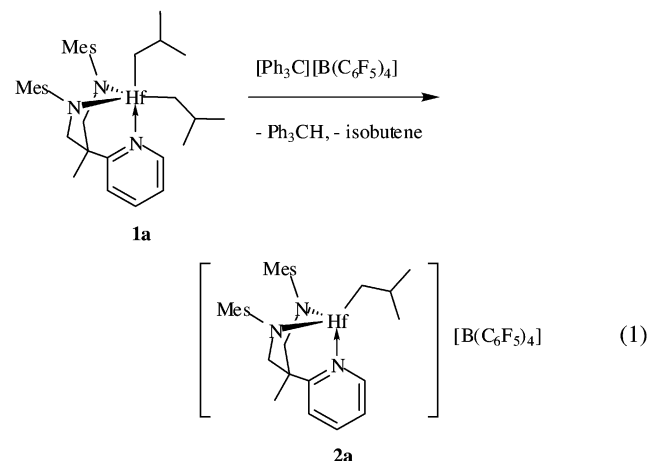
found to have a polydispersity between 1.02 and 1.05 and a molecular weight equal to that expected for a living system.

In this paper we report the full details of the activation of zirconium and hafnium methyl and isobutyl complexes and the living polymerization of 1-hexene by the resulting monoalkyl cations. These results will serve as a base for future investigations of zirconium and hafnium complexes and their use as catalysts for the polymerization of 1-hexene and other olefins. It will be instructive to compare these findings to those obtained with other relatively well-defined “single-site” polymerization catalyst systems based on metallocenes, which until recently<sup>29,30</sup> have not been studied using direct methods.

## Results

**1-Hexene Polymerization with  $\{[\text{MesNpy}]\text{Hf}(\text{i-Bu})\}[\text{B}(\text{C}_6\text{F}_5)_4]$ .** We will begin with a description of the most stable and well-defined cationic monoalkyl complex,  $\{[\text{MesNpy}]\text{Hf}(\text{i-Bu})\}[\text{B}(\text{C}_6\text{F}_5)_4]$  ( $[\text{MesNpy}]^{2-} = [\text{H}_3\text{CC}(2\text{-C}_5\text{H}_4\text{N})(\text{CH}_2\text{N-Mesityl})_2]^{2-}$ ).

Addition of 1 equiv of  $[\text{Ph}_3\text{C}][\text{B}(\text{C}_6\text{F}_5)_4]$  to  $[\text{MesNpy}]\text{Hf}(\text{i-Bu})_2$  (**1a**) or an analogous species in which the isobutyl group is labeled in the  $\alpha$ -position with  $^{13}\text{C}$  (**1a\***) gave (with respect to  $\text{Ph}_3\text{CH}$ ) a quantitative yield of  $\{[\text{MesNpy}]\text{Hf}(\text{i-Bu})\}[\text{B}(\text{C}_6\text{F}_5)_4]$  (**2a** or **2a\***), along with isobutene and  $\text{Ph}_3\text{CH}$  (eq 1). The isobutene was slowly



polymerized in the presence of traces of  $[\text{Ph}_3\text{C}][\text{B}(\text{C}_6\text{F}_5)_4]$ ; isobutene is not polymerized when a different method of activation is employed that generates the  $[\text{HB}(\text{C}_6\text{F}_5)_3]^-$  anion (see later). The  $^{13}\text{C}\{^1\text{H}\}$  NMR spectrum ( $0$  °C,  $\text{C}_6\text{D}_5\text{Br}$ ) of **2a\*** showed a singlet at 93.3 ppm corresponding to the  $\text{Hf-}^{13}\text{CH}_2$  carbon atom (cf. the two  $\alpha$ -carbon resonances at 80.9 and 83.0 ppm in **1a\***). The resonance for  $^{13}\text{CH}_2=\text{C}(\text{CH}_3)_2$  is observed at 111.1 ppm. The  $^1\text{H}$  NMR spectrum ( $-20$  °C,  $\text{C}_6\text{D}_5\text{Br}$ ) for **2a** clearly shows resonances for the methyl, methylene, and methine protons at 0.55, 0.44, and 1.73 ppm, respectively. Variable-temperature  $^{13}\text{C}\{^1\text{H}\}$  NMR studies of **2a\*** show that the isobutyl  $\alpha$ -carbon resonance at 93.3 ppm remains sharp as the temperature of the sample is

(18) Keaton, R. J.; Koterwas, L. A.; Fettinger, J. C.; Sita, L. R. *J. Am. Chem. Soc.* **2002**, *124*, 5932.

(19) Jeon, Y.-M.; Park, S. J.; Heo, J.; Kim, K. *Organometallics* **1998**, *17*, 3161.

(20) Saito, J.; Mitani, M.; Mohri, J.; Yoshida, Y.; Matsui, S.; Ishii, S.; Kojoh, S.; Kashiwa, N.; Fujita, T. *Angew. Chem., Int. Ed.* **2001**, *40*, 2918.

(21) Mitani, M.; Mohri, J.; Yoshida, Y.; Saito, J.; Ishii, S.; Tsuru, K.; Matsui, S.; Furuyama, R.; Nakano, T.; Tanaka, H.; Kohoh, S.; Matsugi, T.; Kashiwa, N.; Fujita, T. *J. Am. Chem. Soc.* **2002**, *124*, 3327.

(22) Mitani, M.; Furuyama, R.; Mohri, J.; Saito, J.; Ishii, S.; Terao, H.; Kashiwa, N.; Fujita, T. *J. Am. Chem. Soc.* **2002**, *124*, 7888.

(23) Mehrkhodavandi, P.; Bonitatebus, P. J., Jr.; Schrock, R. R. *J. Am. Chem. Soc.* **2000**, *122*, 7841.

(24) Mehrkhodavandi, P.; Schrock, R. R. *J. Am. Chem. Soc.* **2001**, *123*, 10746.

(25) Mehrkhodavandi, P.; Schrock, R. R.; Bonitatebus, P. J., Jr. *Organometallics* **2002**, *21*, 5785.

(26) Friedrich, S.; Schubart, M.; Gade, L. H.; Scowen, I. J.; Edwards, A. J.; McPartlin, M. *Chem. Ber. Recl.* **1997**, *130*, 1751.

(27) Blake, A. J.; Collier, P. E.; Gade, L. H.; McPartlin, M.; Mountford, P.; Schubart, M.; Scowen, I. J. *Chem. Commun.* **1997**, 1555.

(28) Schrock, R. R.; Liang, L.-C.; Baumann, R.; Davis, W. M. *J. Organomet. Chem.* **1999**, *591*, 163.

(29) Liu, Z.; Somsok, E.; Landis, C. R. *J. Am. Chem. Soc.* **2001**, *123*, 2915.

(30) Liu, Z.; Somsok, E.; White, C. B.; Rosaaen, K. A.; Landis, C. R. *J. Am. Chem. Soc.* **2001**, *123*, 11193.

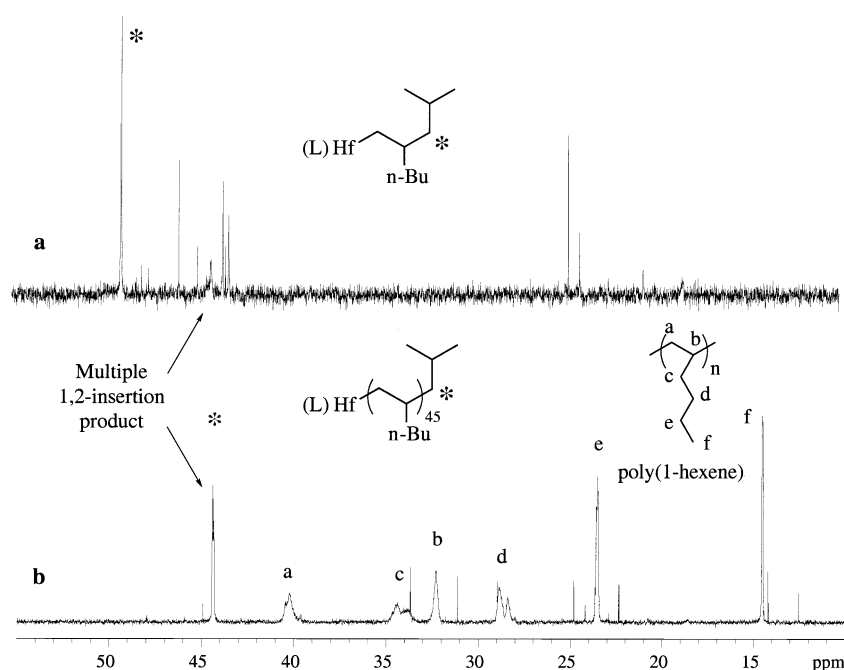


**Figure 1.**  $^{13}\text{C}\{^1\text{H}\}$  NMR spectra ( $0^\circ\text{C}$ ,  $\text{C}_6\text{D}_5\text{Br}$ ) after addition of 1-hexene to **2a**\*: (a) 1–2 equiv of 1-hexene, (b) 45 equiv of 1-hexene; L =  $[\text{MesNpy}]^{2-}$ .

lowered to  $-50^\circ\text{C}$ . Decomposition of **2a** at  $0^\circ\text{C}$  could be followed by observing the decrease in the isobutyl resonance at 0.55 or 0.44 ppm, or both together, over a period of 1 to 2 days. First-order rate constants at  $0^\circ\text{C}$  in bromobenzene was found to be 0.00045, 0.00056, 0.00057, and 0.00060  $\text{min}^{-1}$  for an average of 0.00055–(6)  $\text{min}^{-1}$  or  $9.2(2) \times 10^{-6} \text{ s}^{-1}$ . Isobutene is generated as a product of the decomposition of **2a** and is polymerized irreproducibly in the presence of traces of trityl, as described above. Although we suspect that the immediate organometallic product of the decomposition of **2a** is a cationic hydride complex, we have observed only complex mixtures. Therefore we do not know whether the initial “hydride” simply decomposes further rapidly, even in the presence of 1-hexene, or under some conditions can react with 1-hexene to restart polymer formation. Decomposition of **2a** at  $22^\circ\text{C}$  is complex and depends on metal concentration. The rate of decomposition of **2a** at  $22^\circ\text{C}$  also appears to depend on isobutene concentration, which is present as a product of the initial activation (eq 1) and is also formed upon decomposition of **2a**. The nature of this complex decomposition phenomenon is not understood at this time, so no details are reported here.

Addition of 1–2 equiv of 1-hexene to a solution of **2a**\* leads to a new  $^{13}\text{C}\{^1\text{H}\}$  NMR resonance at 49.0 ppm (\* in Figure 1a). This sharp resonance is attributed to the  $^{13}\text{C}$  label in the first 1,2 insertion product,  $\{[\text{MesNpy}]\text{Hf}(\text{CH}_2\text{CH}(\text{n-Bu})(^{13}\text{CH}_2\text{CHMe}_2))\}[\text{B}(\text{C}_6\text{F}_5)_4]$ . A resonance for the isobutyl  $\alpha$ -carbon atom in unreacted **2a**\* was also observed at 93.3 ppm. Addition of a further 44 equiv of 1-hexene led to the disappearance of the resonance at 93.3 and 49.0 ppm, as well as others, and appearance of a resonance at 44.3 ppm (\* in Figure 1b). Therefore, all of **2a**\* and the first insertion product (and the second, etc.) are converted into multiple 1,2 insertion products whose  $^{13}\text{C}$  labels give rise to the resonance at 44.3 ppm. Natural abundant  $^{13}\text{C}$  resonances for atactic poly(1-hexene) were also observed (Figure 1b).<sup>31,32</sup> No

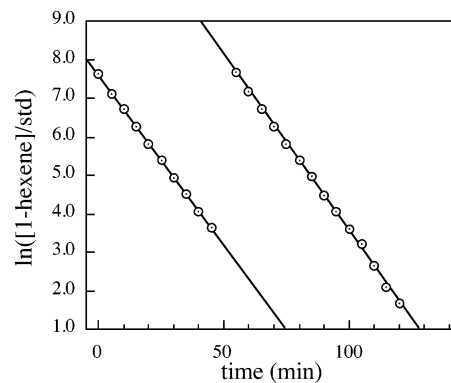


**Figure 2.** Plot of  $\ln[1\text{-hexene}/\text{Ph}_2\text{CH}_2]$  vs time (min) for two consecutive additions of 60 equiv of 1-hexene (0.80 M) to **2a** (0.015 M) ( $0^\circ\text{C}$ ,  $\text{C}_6\text{D}_5\text{Br}$ ).

significant amount of 2,1 insertion into the initial Hf(isobutyl) bond in **2a**\* takes place since no other significant resonance for the  $^{13}\text{C}$  label in the multiple insertion product was found. Since the reaction of the isobutyl species is a close analogue for the propagation reaction, we propose that the propagating species reacts with 1-hexene primarily, if not solely, to give 1,2 insertion products. This is supported further by the nature of the olefin formed upon  $\beta$ -hydride elimination from the propagating species (see below).

The disappearance of 1-hexene in the presence of **2a** at  $0^\circ\text{C}$  in  $\text{C}_6\text{D}_5\text{Br}$  was found to follow first-order kinetics (versus an internal standard,  $\text{Ph}_2\text{CH}_2$ ), as shown in Figure 2. (The 1-hexene that was employed contained  $\sim 0.1\%$  of a  $\text{H}_2\text{C}=\text{CRR}'$  species with vinylidene proton resonances that are coincident with those in 2-methyl-1-pentene. Neither the 2-methyl-1-pentene impurity nor the isobutene generated in the activation step reacted

(31) Asakura, T.; Demura, M.; Nishiyama, Y. *Macromolecules* **1991**, *24*, 2334.

(32) Babu, G. N.; Newmark, R. A.; Chien, J. C. *Macromolecules* **1994**, *27*, 3383.

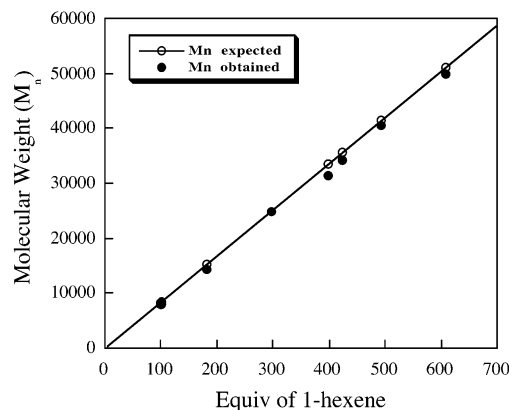
**Table 1. Summary of the Propagation Rate Constants for Polymerization of Various  $\alpha$ -Olefins by **2a** in  $C_6D_5Br$  at 0 °C**

olefin	$k_p$ ( $M^{-1} s^{-1}$ )
1-hexene	0.10(1)
1-octene	0.13(1)
1-decene	0.14(1)
1-tetradecene	0.15(1)
3-methyl-1-pentene	$7.2 \times 10^{-4}$
4,4-dimethyl-1-pentene	$6.2 \times 10^{-3}$

with the cationic hafnium alkyl.) Two consecutive additions of 60 equiv of 1-hexene to a solution of **2a** in  $C_6D_5Br$  at 0 °C resulted in linear plots of  $\ln[1\text{-hexene}]$  versus time. If  $d[1\text{-hexene}]/dt = -k_p[Hf]_0[1\text{-hexene}]$ ,  $k_p = 6.0(2) M^{-1} \text{min}^{-1}$  ( $0.10(2) M^{-1} s^{-1}$ ). The rate of 1-hexene polymerization with **2a** was monitored (in 6 runs) over catalyst concentrations in the range 8–23 mM. The values for  $k_{obs}$  in these runs were found to correlate directly with  $[Hf]_0$ , as expected. Propagation rate constants obtained over this concentration range resulted in an average  $k_p$  value of  $6.0(6) M^{-1} \text{min}^{-1}$  ( $0.10(1) M^{-1} s^{-1}$ ) at 0 °C (Table 1).

The polymerization of 1-hexene by **2a** is well-behaved at 10 °C or below with  $k_p$  values (in  $M^{-1} s^{-1}$  at degrees K) equal to 0.020 (253 K), 0.049 (263 K), 0.065 (268 K), 0.098 (273 K), and 0.16 (278 K) at  $[Hf]_0$  concentrations near 15 mM. (The catalyst concentration was determined in situ by integration versus an internal standard.) An Eyring plot ( $R = 0.997$ ) of  $\ln(k/T)$  vs  $1/T$ , where  $k$  is the theoretical first-order rate constant and  $[Hf]_0$  is set at 1 M, yielded  $\Delta H^\ddagger = 10.82 \text{ kcal mol}^{-1}$  and  $\Delta S^\ddagger = -23.01 \text{ cal mol}^{-1} \text{K}^{-1}$ . The relatively large and negative  $\Delta S^\ddagger$  is consistent with a rate-limiting bimolecular propagation step.

Up to 600 equiv of 1-hexene were polymerized by **2a** in chlorobenzene in a series of batchwise experiments that were carried out for 2 h at 0 °C. (The half-life of 1-hexene at a catalyst concentration of 0.015 M is 7.7 min. Therefore all 1-hexene is polymerized in ~40 min at 0 °C.) The molecular weights and polydispersities of these samples were determined by GPC using a combination of light-scattering and refractometer GPC data. (The value for  $dn/dc$  determined by the manufacturer of the light-scattering instrument (Wyatt) on atactic poly(1-hexene) samples prepared in our laboratory using **2a** was found to be 0.076; this value was employed in molecular weight measurements.) The plot of  $M_n$  versus the number of equivalents employed was linear over the range 100 to ~600 equiv, and polydispersity values were between 1.02 and 1.05 (Figure 3; Table 2). In one experiment, 91 equiv of 1-hexene were added to a solution of **2a** (8.8 mM,  $C_6D_5Br$ ). After 2 h at 0 °C another 91 equiv of 1-hexene were added and polymerization resumed at 0 °C for another 2 h. The resulting polymer sample had a PDI = 1.04 and  $M_n = 13\,650$  (theoretical  $M_n = 15\,320$ ), which is within the error limit for molecular weight determinations of this type in this range. These data suggest that little catalyst decomposes (e.g., by  $\beta$ -hydride elimination) during this time period. Unfortunately, we have not been able to find an NMR resonance that is unique for the living species and, therefore, have not been able to measure the rate of its decomposition directly at 0 °C. If we say that the rate of decomposition of **2a** is approximately the same as the rate of decomposition of the living polymer, then in 2 h

**Figure 3.** Analysis of poly(1-hexene) obtained employing **2a** (0 °C,  $C_6H_5Cl$ ). Polydispersity values are between 1.02 and 1.05 (see Table 1).**Table 2. Characteristics of Poly(1-hexene) Prepared Employing Various Dialkyls Activated with  $[Ph_3C][B(C_6F_5)_4]$  at 0 °C in Chlorobenzene or  $C_6D_5Br^a$** 

dialkyl complex	conc (mM)	olefin (equiv)	$M_n$ theory	$M_n$ found	fd/th	PDI
$[MesNpy]Hf(i-Bu)_2$	10.6	98	8248	8012	0.97	1.04
	9.7	101	8500	7888	0.93	1.04
	5.3	182	15 317	14 380	0.94	1.04
	5.1	296	24 911	24 800	1.00	1.03
	5.7	398	33 496	31 370	0.94	1.03
	2.7	423	35 600	34 220	0.96	1.02
$[MesNpy]Zr(i-Bu)_2$	5.2	493	41 491	40 610	0.98	1.03
	4.9	607	51 085	49 970	0.98	1.03
	15	107	9005	9092	1.00	1.03 <sup>a</sup>
$[MesNpy]ZrMe_2$	7.3	220	18 515	19 190	1.04	1.02 <sup>a</sup>
	1.2	63	5300	60 000	11.3	1.02
	1.0	77	6480	65 000	10.0	1.07

<sup>a</sup> In  $C_6D_5Br$  at 0 °C after NMR studies (see Experimental Section).

at 0 °C only ~4% of the propagating species would have decomposed. As noted above all 1-hexene is polymerized at 40 min at 0 °C, so decomposition of the living polymer is likely to be negligible during this period, as is also suggested by the data in Figure 3.

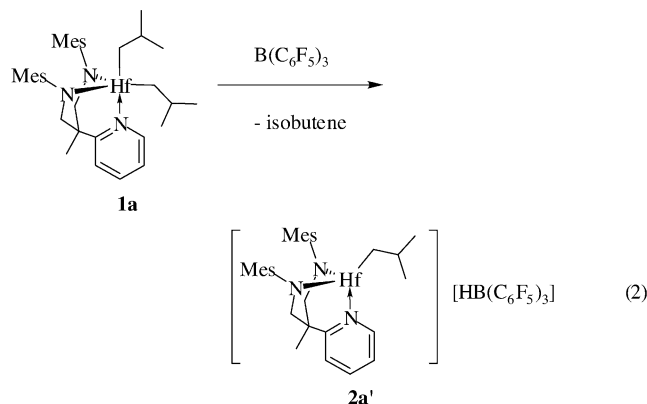
No resonances at 4.83 and 4.85 ppm or between 5.3 and 5.5 ppm were observed in polymerization runs of up to 600 equiv of 1-hexene at 0 °C. However, if polymerization reactions that are completed at 0 °C are allowed to warm to room temperature, then olefinic resonances characteristic of  $\beta$ -elimination from a 1,2 insertion product appear at 4.83 and 4.85 ppm.<sup>33,34</sup> No resonances at 5.3–5.5 ppm characteristic of an internal olefin (the product of  $\beta$ -elimination from a 2,1 insertion product<sup>33,34</sup>) were observed. This confirms that the chain end that is present results from a 1,2 insertion. The  $\beta$ -(1,2) elimination product was observed to grow in with time. Unfortunately, a rate for forming this product could not be obtained since it was polymerized slowly (along with isobutene) in the presence of traces of trityl. Addition of 100 equiv of 1-hexene to an initially cold (–20 °C) solution of **2a** followed by warming the sample to room temperature as the polymerization was com-

(33) Moscardi, G.; Resconi, L.; Cavallo, L. *Organometallics* **2001**, *20*, 1918.

(34) Resconi, L.; Piemontesi, F.; Camurati, I.; Sudmeijer, O.; Nifant'ev, I. E.; Ivchenko, P. V.; Kuz'mina, L. G. *J. Am. Chem. Soc.* **1998**, *120*, 2308.

pleted led to polymer samples with PDI = 1.04 and  $M_n = 7500$  (expected  $M_n = 8420$ ). Addition of 100 equiv of 1-hexene to this sample at room temperature led to polymers that clearly showed bimodal GPC traces (by both refractive index and light-scattering methods), consistent with significant chain termination by  $\beta$ -hydride elimination before and during renewed chain growth at room temperature at the concentrations of 1-hexene employed.

Activation of **1a**\* with  $B(C_6F_5)_3$  led to clean abstraction of a  $\beta$ -hydride and formation of  $\{[MesNpy]Hf(^{13}CH_2CHMe_2)[HB(C_6F_5)_3]\}$  (**2a**\*) as well as  $^{13}CH_2=C(CH_3)_2$  (eq 2). The  $^1H$  and  $^{13}C\{^1H\}$  NMR spectra (0 °C,



$C_6D_5Br$ ) of **2a**' show resonances for the Hf-CH<sub>2</sub> protons and  $\alpha$ -carbon at 0.4 and 94.0 ppm, respectively, which are close to those reported for **2a**\*. The  $^1H$  NMR resonance for the proton attached to boron in  $[HB(C_6F_5)_3]^-$  could not be found. The only byproduct of the reaction is isobutene, which is *not* polymerized over a period of 24 h at room temperature. (In contrast, activation of diisobutyl complexes with  $[Ph_3C][B(C_6F_5)_4]$  results in polymerization of isobutene in the presence of traces of  $[Ph_3C][B(C_6F_5)_4]$  at 0 °C.) In contrast to decomposition of **2a** (vide supra) decomposition of **2a**' at 22 °C proceeded in a first-order manner with  $k_d = 0.0044$  (2 runs) and  $0.0045 \text{ min}^{-1}$  for an average  $k_d = 0.0044(1) \text{ min}^{-1}$  or  $7.3(2) \times 10^{-5} \text{ s}^{-1}$  (3 runs total). At 0 °C  $k_d = 2.8 \times 10^{-6} \text{ s}^{-1}$ , which is roughly one-third the rate of decomposition of **2a**.

Polymerization of 1-hexene by **2a**' in  $C_6D_5Br$  at 0 °C was well-behaved with  $k_p = 0.048(1) \text{ M}^{-1} \text{ s}^{-1}$  (Figure 4). This should be compared with  $k_p = 0.10(1) \text{ M}^{-1} \text{ s}^{-1}$  for the  $[B(C_6F_5)_4]^-$  salt. Since compound **2a**' is sparingly soluble in toluene (**2a** is essentially insoluble in toluene), 1-hexene polymerization with **2a**' also could be carried out in toluene, in which  $k_p = 0.0111(3) \text{ M}^{-1} \text{ s}^{-1}$  (Figure 4), a further reduction of  $k_p$  by approximately a factor of 4 compared to bromobenzene and approximately 1 order of magnitude less than  $k_p$  for the  $[B(C_6F_5)_4]^-$  salt in bromobenzene (Table 2).

**Polymerization of Other Terminal Olefins.** Polymerizations of several other terminal olefins were examined. The polymerization of 1-octene was carried out with **2a** concentrations ranging from 7.5 to 28 mM over 6 runs at 0 °C in bromobenzene. The value for  $k_p$  was found to be  $7.7(3) \text{ M}^{-1} \text{ min}^{-1}$ . In seven trials with **2a** concentrations ranging from 7 to 27 mM, it was determined that the average  $k_p$  for 1-decene was  $8.4(4) \text{ M}^{-1} \text{ min}^{-1}$ . The polymerization of 1-tetradecene was

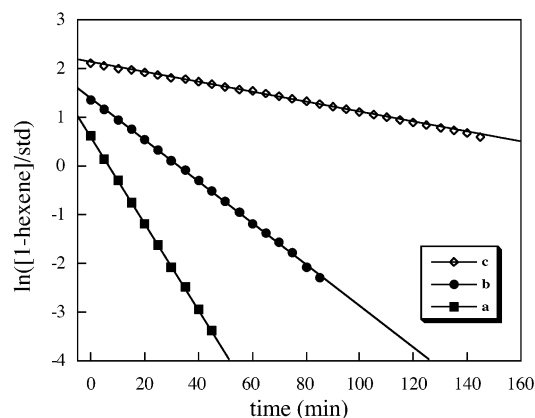
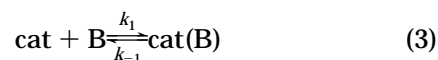


**Figure 4.** Plots of  $\ln([1\text{-hexene}]/Ph_2CH_2)$  vs time (min) after addition of 1-hexene to  $[(MesNpy)Hf(i-Bu)][A]$  (~15 mM) (0 °C, S): (a)  $A = [B(C_6F_5)_4]^-$ ,  $S = C_6D_5Br$ ; (b)  $A = [HB(C_6F_5)_3]^-$ ,  $S = C_6D_5Br$ ; (c)  $A = [HB(C_6F_5)_3]^-$ ,  $S = C_6D_5-CD_3$ .

monitored over 6 runs at a **2a** concentration range of 7–27 mM; the average  $k_p$  was  $9.1(3) \text{ M}^{-1} \text{ min}^{-1}$ . All data are gathered in Table 1 in units of  $\text{M}^{-1} \text{ s}^{-1}$ . At this stage we do not want to make much of the small increase in  $k_p$  with increasing chain length.

Polymerizations of both 3-methyl-1-pentene and 4,4-dimethyl-1-pentene at 0 °C were very much slower than unbranched terminal olefins, with  $k_p = 7.2 \times 10^{-4} \text{ s}^{-1}$  for the former and  $6.2 \times 10^{-3} \text{ s}^{-1}$  for the latter. (Both are single runs.) The rate of polymerization of 3-methyl-1-pentene is more than 100 times slower than 1-hexene. We ascribe the slower rates to bulk steric effects, with the effect being greater for substitution closer to the double bond.

**Well-Behaved Inhibitors for 1-Hexene Polymerization.** It has been known for some time in single-site cationic group 4 catalyst systems in general that polymerization is quenched in the presence of donors such as diethyl ether. We find too that polymerization of 1-hexene is quenched after addition of even stoichiometric quantities of diethyl ether or THF to the cations. For example, 4 equiv of diethyl ether were added to a 22 mM solution of **2a** in bromobenzene and 72 equiv of 1-hexene were added; no polymer was observed at 0 °C after 2 h. However, if the catalysts are as well-behaved as they appear to be, then we should be able to find some (larger) bases that will bind to the metal with a strength approximately the same as that of the olefin. If we make the assumption that an inhibitor binds to the cationic catalyst to yield an inactive base adduct (cat(B), eq 3), that the “on” and “off” rates for the base are both fast with respect to insertion of olefin into the metal–carbon bond in the base-free catalyst (cat), and that  $[cat]_0 = [cat] + [cat(B)]$ , then  $k_{obs} = k_p[cat]_0/(1 + K[B])$ , which is rewritten as eq 4. A plot of  $[cat]_0/k_{obs}$  versus  $[B]$  then should give a line with slope  $K/k_p$  and intercept  $1/k_p$ , from which both  $K$  and  $k_p$  can be extracted. The value of  $k_p$  ( $0.10 \text{ M}^{-1} \text{ s}^{-1}$ ) is known in this case by direct measurement in the absence of inhibitor.



$$\frac{[cat]_0}{k_{obs}} = \frac{K}{k_p}[B] + \frac{1}{k_p} \quad (4)$$

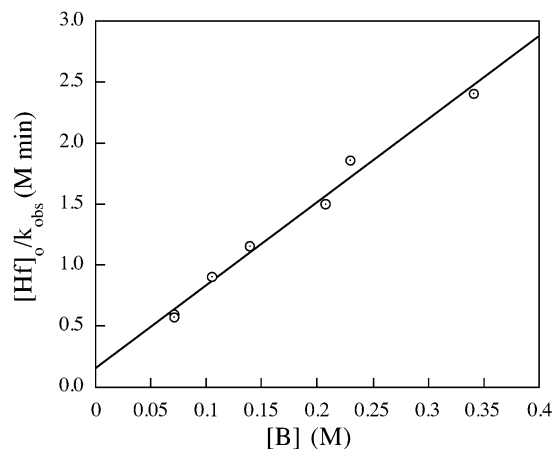


**Figure 5.** Plot of  $[\text{Hf}]_0/k_{\text{obs}}$  (M min) vs  $[\text{B}]$  for polymerization of 1-hexene by **2a** (~15 mM) in the presence of  $(i\text{-Pr})_2\text{O}$  (0 °C,  $\text{C}_6\text{D}_5\text{Br}$ ).

Diisopropyl ether was the first well-behaved base to be discovered. A plot of  $[\text{Hf}]_0/k_{\text{obs}}$  vs  $[\text{B}]$  (Figure 5) produced a value for  $k_p$  of  $0.11(1) \text{ M}^{-1} \text{ s}^{-1}$  and a  $K = 41(5) \text{ M}^{-1}$ . The derived value for  $k_p$  agrees with the experimental value of  $0.10(1) \text{ M}^{-1} \text{ s}^{-1}$ , which technically could also be employed as a point (where  $[\text{B}] = 0$ ) in the plot in Figure 5. In one experiment the rate of polymerization of 52 equiv of 1-hexene by **2a** was first determined, then 14 equiv of  $(i\text{-Pr})_2\text{O}$  were added to the same solution, and another 52 equiv of 1-hexene were added. The resulting decrease in the slope of  $\ln[1\text{-hexene}]$  versus time was that predicted on the basis of the above analysis. Polymerization of a bulk sample (141 equiv of 1-hexene) in the presence of 13 equiv of  $(i\text{-Pr})_2\text{O}$  gave a polymer sample with  $\text{PDI} = 1.05$  and  $M_n = 11\,900$  (expected  $M_n = 11\,870$ ). These data suggest that the presence of diisopropyl ether is not deleterious in any way to the polymerization, except in rate; that is, it is a well-behaved inhibitor. As noted above, polymerizations are quenched at 0 °C upon addition of  $\geq 1$  equiv of diethyl ether.

Polymerization of 1-hexene was examined in the presence of  $(\text{TMS})_2\text{O}$  (114 equiv relative to catalyst = 14 mM). The value for  $k_p$  was the same as in the absence of  $(\text{TMS})_2\text{O}$ . However, polymerization of 1-hexene at 0 °C was inhibited by hexyltrimethylsilyl ether, with a  $K = 220 \text{ M}^{-1}$  being determined in runs in the presence of 10, 30, and 100 equiv of hexyltrimethylsilyl ether. This  $K$  is roughly 5 times the  $K$  value for diisopropyl ether.

Triethylamine and tributylamine also proved to be well-behaved inhibitors. Polymerization of 1-hexene with **2a** in the presence of  $\text{NEt}_3$  proceeded with first-order kinetics and no observable initiation period. A plot of  $[\text{Hf}]_0/k_{\text{obs}}$  versus  $[\text{B}]$  was linear and gave a  $K$  value of  $73(7) \text{ M}^{-1}$ . Polymerization of 247 equiv of 1-hexene with a 10 mM solution of **2a** (0 °C,  $\text{C}_6\text{H}_5\text{Cl}$ ) with 9 equiv  $\text{NEt}_3$  resulted in a polymer sample with  $M_n = 22\,900$  ( $M_n$  expected = 20 790) and  $\text{PDI} = 1.08$ . Tributylamine was actually a slightly *more* efficient inhibitor than triethylamine. The linear plot of  $[\text{Hf}]_0/k_{\text{obs}}$  versus  $[\text{B}]$  showed a  $K$  value of  $107(11) \text{ M}^{-1}$ .

Polymerization of 115 equiv of 1-hexene ( $[1\text{-hexene}]_0 = 1.50 \text{ M}$ ) by a mixture of **2a** (0.13 M) and 20 equiv of dimethylaniline (0.26 M) resulted in a *nonlinear* plot of  $\ln([1\text{-hexene}]/\text{std})$  versus time over several half-lives.

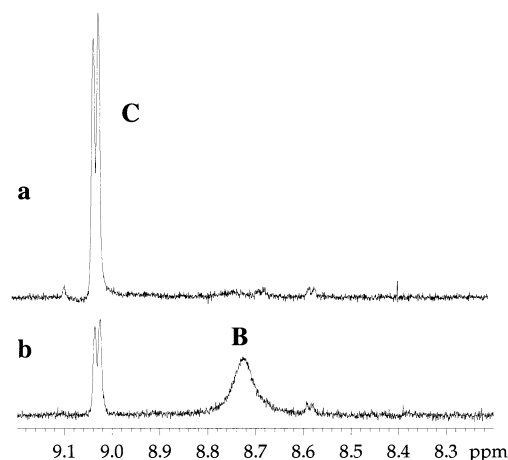
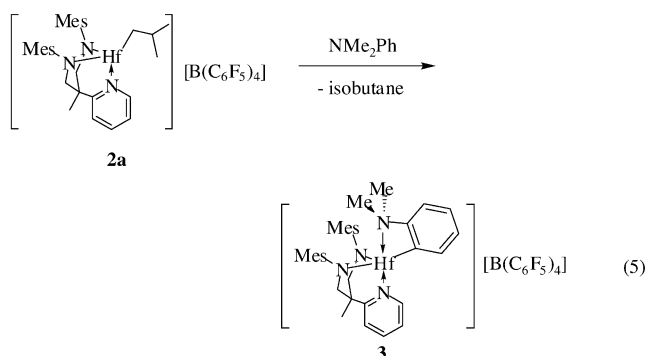


**Figure 6.**  $^1\text{H}$  NMR spectra (0 °C,  $\text{C}_6\text{D}_5\text{Br}$ ) for the *ortho* pyridyl region after addition of  $\text{NMe}_2\text{Ph}$  (18 equiv) and 1-hexene (100 equiv) to  $\{[\text{MesNpy}]\text{Hf}(i\text{-Bu})\}[\text{B}(\text{C}_6\text{F}_5)_4]$  (0.013M) (b) ~10 min after mixing and (a) 2 h later.

Proton NMR spectra during polymerization revealed that the sharp pyridyl  $\text{H}_o$  resonance for **2a** at 8.39 ppm had been replaced by a broad pyridyl  $\text{H}_o$  resonance at 8.72 ppm characteristic of the propagating species (**B** in Figure 6b), as expected, although a new, sharp resonance began to appear at 9.03 ppm (**C** in Figure 6) over a period of 2 h. The 9.03 ppm resonance must be ascribed to a nonpolymeric species, since it is sharp, as in **2a**. Resonances corresponding to vinylidene protons were not observed; that is, chain termination via  $\beta$ -hydride elimination did not take place. We propose that the new  $\text{H}_o$  resonance is that in a species formed in a reaction between the propagating species and dimethylaniline (**3** in eq 5). The disappearance of the resonance at 8.72 ppm was found to be first-order with  $k = 4.5 \times 10^{-4} \text{ s}^{-1}$  or a second-order rate constant for the reaction between the living species and dimethylaniline ( $k_{\text{AN}}$ ) of  $1.7 \times 10^{-4} \text{ M}^{-1} \text{ s}^{-1}$ . The time required to consume 50% of the initial 1-hexene at 0 °C when  $[\text{Hf}] = 0.013 \text{ M}$  is ~9 min. During that time ~20% of the living species would have reacted with dimethylaniline (if  $[\text{dimethylaniline}]_0 = 0.26 \text{ M}$ ). In 2 h ~75% of the living species would be consumed. These data are consistent with the observations shown in Figure 6. It should be noted that if the aniline concentration is equal to the catalyst concentration, then the initial rate of reaction of aniline with the living polymer is only 1/20 as fast. In fact, reactions in which the  $[\text{B}(\text{C}_6\text{F}_5)_4]^-$  salt of dimethylanilinium was employed as an initiator showed only a few percent of **3**. Therefore the  $[\text{B}(\text{C}_6\text{F}_5)_4]^-$  salt of dimethylanilinium can be a relatively well-behaved initiator for 1-hexene polymerization, depending upon the circumstances, even though dimethylaniline is a poorly behaved inhibitor at high concentrations. Addition of 1-hexene to samples containing only **3** led to essentially no poly(1-hexene) being formed at 0 °C, i.e., **3** is inactive.

Complex **2a** itself was found to react with dimethylaniline to yield a species with the same pyridyl resonance at 9.03 ppm in the proton NMR spectrum. The reaction between **2a** (0.022 M) and dimethylaniline (0.99 M) was found to be (pseudo) first-order with a first-order rate constant  $k_d = 1.11(2) \times 10^{-4} \text{ s}^{-1}$  ( $t_{1/2} = 104 \text{ min}$  at this concentration of dimethylaniline) or a second-order

$k = 1.1 \times 10^{-4} \text{ M}^{-1} \text{ s}^{-1}$  at  $0^\circ \text{C}$ , which is slightly smaller than that for the reaction between the living polymer and dimethylaniline. (The reaction was followed by monitoring the disappearance of the ligand backbone resonance for **2a** at 4.4 ppm in the  $^1\text{H}$  NMR spectrum.) When **2a\*** was employed, the  $^{13}\text{C}\{^1\text{H}\}$  NMR spectrum showed resonances for  $^{13}\text{CH}_2=\text{C}(\text{CH}_3)_2$  (at 111.14 ppm) from the initial activation process, **2a\*** (at 94.22 ppm, cf. at 93.3 ppm in the base-free species), and  $^{13}\text{CH}_3\text{CH}(\text{CH}_3)_2$  (at 24.82 ppm). The formation of isobutane is consistent with the proposed CH activation process (eq 5).

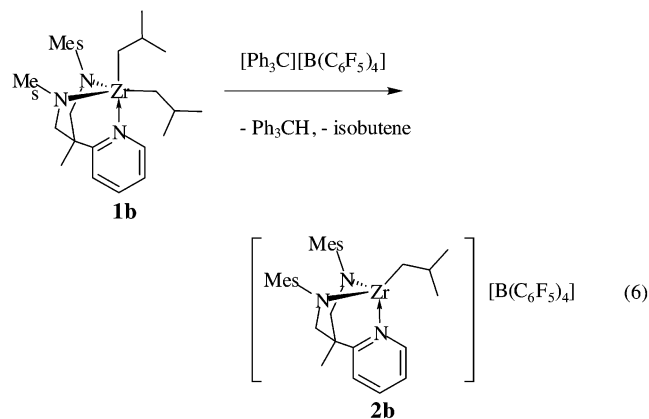


A compound analogous to **3** was synthesized at  $0^\circ \text{C}$  over a 24 h period by adding 1 equiv of  $\text{NMe}_2\text{Ph}$  to  $\{[\text{MesNpy}]\text{Hf}(\text{i-Bu})\}[\text{HB}(\text{C}_6\text{F}_5)_3]$ . It was isolated as a yellow powder in 72% yield and was characterized by elemental analysis as well as various NMR spectroscopic methods. The  $^1\text{H}$  NMR spectrum ( $20^\circ \text{C}$ ,  $\text{C}_6\text{D}_5\text{Br}$ ) is essentially identical to that obtained for the decomposition product during polymerization of 1-hexene in the presence of dimethylaniline. A gCOSY experiment allowed a full assignment of the spectrum. Three resonances in the aliphatic region were attributed to methyl groups of the mesityl ring. The fourth resonance at 2.13 ppm is assigned to the  $\text{N-CH}_3$  groups of a C-H activated dimethylaniline. Resonances for the four protons of the  $\text{N-C}_6\text{H}_4$  ring were also observed and assigned. The  $^{13}\text{C}\{^1\text{H}\}$  NMR spectrum shows a resonance at 47.9 ppm for the  $\text{N-CH}_3$  carbon atom. All NMR data can be found in the Experimental Section. Unfortunately, no crystals suitable for an X-ray structural study could be obtained.

Diphenyl ether was also unsuitable as an inhibitor at high concentrations ( $\sim 20\times$  the catalyst concentration of  $\sim 0.15 \text{ M}$ ) as a consequence of what we assume to be a CH activation related to that found for dimethylaniline. In addition to the broad resonance for the pyridyl proton in the propagating species, two sets of sharp doublets at 8.70 and 8.74 ppm were observed to grow in during the polymerization reaction. Therefore we believe that CH activation in diphenyl ether takes place to yield two different products, the precise nature of which is not known. For this reason we did not explore inhibition by diphenyl ether further.

We conclude that well-behaved inhibitors can be found, although CH activation in phenyl rings that are directly attached to the coordinating atom in the base appear to be a complication (at least for 1-hexene under the conditions employed) that can compromise the living nature of the polymerization process at relatively high concentrations of added base.

**Polymerization of 1-Hexene with Activated  $[\text{MesNpy}]\text{Zr}(\text{i-Bu})_2$ .** Although  $[\text{MesNpy}]\text{Zr}(\text{i-Bu})_2$  (**1b**) is thermally unstable and sensitive to light,<sup>25</sup> it can be activated with 1 equiv of  $[\text{Ph}_3\text{C}][\text{B}(\text{C}_6\text{F}_5)_4]$  (at  $-20^\circ \text{C}$  in  $\text{C}_6\text{D}_5\text{Br}$ ) to give  $\{[\text{MesNpy}]\text{Zr}(\text{i-Bu})\}[\text{B}(\text{C}_6\text{F}_5)_4]$  (**2b**) (eq 6) quantitatively. The  $^1\text{H}$  and  $^{13}\text{C}\{^1\text{H}\}$  NMR spectra



( $-30^\circ \text{C}$ ,  $\text{C}_6\text{D}_5\text{Br}$ ) of **2b** show only one set of peaks corresponding to the isobutyl's  $\alpha$ -methylene protons (at 0.62 ppm) and carbon atom (at 83.3 ppm). Compound **2b** decomposes at  $0^\circ \text{C}$  to give isobutene and a complex mixture of products. Decomposition was followed by  $^1\text{H}$  NMR spectroscopy ( $0^\circ \text{C}$ ,  $\text{C}_6\text{D}_5\text{Br}$ ) with respect to an internal standard ( $\text{Ph}_2\text{CH}_2$ ) and was found to be first-order over several half-lives. However, the rate constant that was obtained varied significantly from batch to batch of **1b**, with values  $k_d = 6.7 \times 10^{-6}$ ,  $9.8 \times 10^{-6}$ ,  $1.5 \times 10^{-5}$ , and  $3.0 \times 10^{-5} \text{ s}^{-1}$  being obtained, with more rapid decompositions of **2b** being recorded when the initiator was prepared from progressively older samples of **1b**. (Samples of **1b** were stored at  $-30^\circ \text{C}$  in the dark.) The reason for more rapid decompositions of **2b** from "aged" samples of **1b** is not known. As decomposition of **2b** progresses, the concentration of isobutene in solution increases, but then decreases as (we believe) it is polymerized in the presence of traces of  $[\text{Ph}_3\text{C}][\text{B}(\text{C}_6\text{F}_5)_4]$ . The decomposition is believed to proceed via  $\beta$ -hydride elimination to yield isobutene; the zirconium product of the decomposition could not be determined. If **2b** is prepared at  $0^\circ \text{C}$  or below and kept at that temperature, then virtually none decomposes before 1-hexene is added.

Addition of 100 equiv of 1-hexene to **2b** (6.8 mM) in  $\text{C}_6\text{D}_5\text{Br}$  led to a plot of  $\ln[1\text{-hexene}]$  versus time that was linear over several half-lives at  $-20$ ,  $-10$ ,  $0$ , and  $10^\circ \text{C}$ . The respective  $k_p$  values were 0.027, 0.044, 0.084, and  $0.16 \text{ M}^{-1} \text{ s}^{-1}$ , respectively. An Eyring plot (for  $[\text{Zr}] = 1 \text{ M}$ ) led to  $\Delta H^\ddagger = 8.09 \text{ kcal mol}^{-1}$  and  $\Delta S^\ddagger = -33.34 \text{ cal mol}^{-1} \text{ K}^{-1}$ . A comparison of  $k_p$  for  $\{[\text{MesNpy}]\text{Zr}(\text{i-Bu})\}[\text{B}(\text{C}_6\text{F}_5)_4]$  ( $0.084 \text{ M}^{-1} \text{ s}^{-1}$ ) with that for  $\{[\text{MesNpy}]\text{Hf}(\text{i-Bu})\}[\text{B}(\text{C}_6\text{F}_5)_4]$  ( $0.10 \text{ M}^{-1} \text{ s}^{-1}$ ) reveals that they are virtually identical. The polymerization at  $0^\circ \text{C}$  was repeated with a different batch of catalyst by a second individual; the result was  $k_p = 0.097 \text{ M}^{-1} \text{ s}^{-1}$ .

As shown in Table 1, the molecular weights of the polymers obtained with **2b** as a catalyst were those expected for a living system. It should be noted, however, that higher than expected molecular weights have been observed if the catalyst is not freshly prepared and if the reactions are not quenched with methanol im-

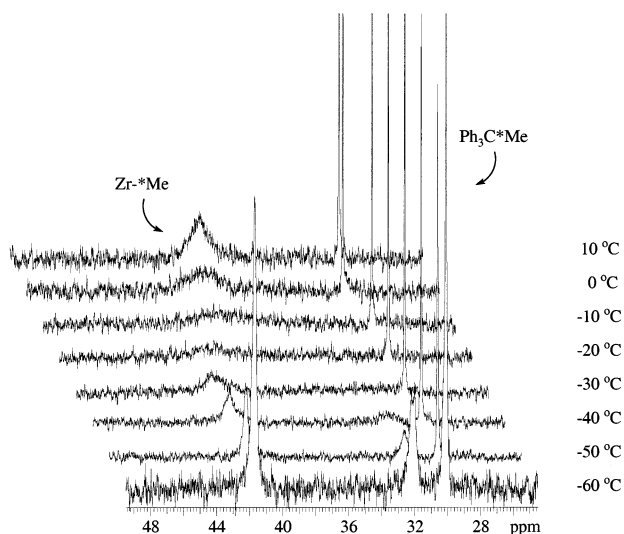


**Figure 7.** Variable-temperature  $^{13}\text{C}\{^1\text{H}\}$  NMR spectra (1:1  $\text{C}_6\text{D}_5\text{Br}:\text{C}_6\text{D}_5\text{CD}_3$ ) of  $[\text{MesNpy}]\text{Zr}^{13}\text{Me}_2$  activated with  $[\text{Ph}_3\text{C}][\text{B}(\text{C}_6\text{F}_5)_4]$  (1.0 equiv).

mediately after they are complete. Variable results of this nature confirm that polymerizations by **2b** are potentially much more problematic than polymerizations by **2a**.

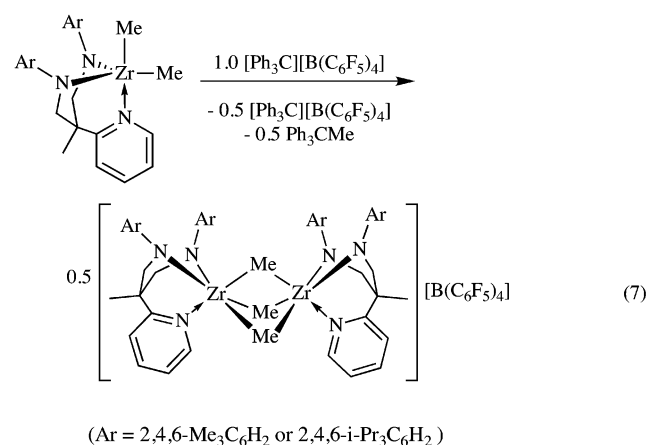
**Activation of  $[\text{ArNpy}]\text{ZrMe}_2$  and Labeling Studies.** Activation of  $[\text{MesNpy}]\text{ZrMe}_2$  (**4**) with 1.0 equiv of  $[\text{Ph}_3\text{C}][\text{B}(\text{C}_6\text{F}_5)_4]$  (20 °C,  $\text{C}_6\text{D}_5\text{Br}$ ) results in formation of  $\text{Ph}_3\text{CMe}$  and a zirconium cation (**5**). An  $^1\text{H}$  NMR spectrum of this cation shows a sharp resonance at 2.03 ppm, which corresponds to the three protons of  $\text{Ph}_3\text{CCH}_3$ , and a broader resonance at 0.66 ppm, which corresponds to approximately nine protons, i.e., three methyl groups are present in this cation. In the  $^1\text{H}$  NMR spectrum of activated  $[\text{MesNpy}]\text{Zr}^{13}\text{Me}_2$  (**4\***, which yields **5\***) the methyl resonance splits into two resonances with a  $J_{\text{CH}}$  of 108 Hz, while the  $^{13}\text{C}\{^1\text{H}\}$  NMR spectrum shows a broad singlet at 38 ppm at room temperature (Figure 7).

Variable-temperature  $^{13}\text{C}\{^1\text{H}\}$  NMR studies of **5\*** were carried out in a 1:1 mixture of  $\text{C}_6\text{D}_5\text{Br}$  and  $\text{C}_6\text{D}_5\text{CD}_3$  (Figure 7). These studies show that as the solution is cooled to  $-60$  °C, the resonance at 38 ppm broadens and splits into two peaks (at 41.9 and 32.1 ppm) in a 2:1 ratio. A proton-coupled  $^{13}\text{C}$  NMR experiment at  $-60$  °C showed the  $J_{\text{CH}}$  for both resonances to be 108 Hz. The three methyl groups therefore are likely to be of the same type. A  $^1\text{H}$  ROESY experiment ( $-25$  °C,  $\text{C}_6\text{D}_5\text{Br}$ ) shows NOE cross-peaks between the  $\text{Zr}-\text{CH}_3$  and the *ortho* pyridyl proton resonances and between  $\text{Zr}-\text{CH}_3$  and one set of the mesityl *ortho* methyl groups.

Activation of  $[\text{TripNpy}]\text{ZrMe}_2$  (**6**) with 1 equiv of  $[\text{Ph}_3\text{C}][\text{B}(\text{C}_6\text{F}_5)_4]$  (Trip = 2,4,6-triisopropylphenyl) results in formation of  $\text{Ph}_3\text{CMe}$  and a cationic species (**7**) that is similar to **5**. The  $^1\text{H}$  NMR spectrum of **7** (20 °C,  $\text{C}_6\text{D}_5\text{Br}$ ) shows a single broad peak at 0.9 ppm corresponding to the  $\text{Zr}-\text{CH}_3$  group, with a  $J_{\text{CH}}$  value of 109 Hz. Variable-temperature studies of the  $^{13}\text{C}$ -labeled cation (obtained from activation of **6\***) in a 1:1 mixture of  $\text{C}_6\text{D}_5\text{Br}$  and  $\text{C}_6\text{D}_5\text{CD}_3$  reveal two resonances at  $-70$  °C (at 47.2 and 36.3 ppm) in a 1:2 ratio. In **7** the most upfield  $\text{Zr}-^{13}\text{Me}$  resonance is that ascribed to the two

equivalent methyl groups, while in **5** the downfield resonance is that ascribed to the two equivalent methyl groups.

Observation of **5** and **7** suggests that activation of  $[\text{ArNpy}]\text{ZrMe}_2$  complexes with 1.0 equiv of  $[\text{Ph}_3\text{C}][\text{B}(\text{C}_6\text{F}_5)_4]$  does not result in formation of the expected  $\{[\text{ArNpy}]\text{ZrMe}\}[\text{B}(\text{C}_6\text{F}_5)_4]$  species in a readily observable amount. On the basis of formation of structurally characterized  $\{[\text{MesN}_2\text{NMe}]_2\text{Zr}_2\text{Me}_3\}^+$  (where  $[\text{MesN}_2\text{NMe}]^{2-} = [(\text{MesNCH}_2\text{CH}_2)_2\text{NMe}]^{2-}$ ),<sup>35</sup> we propose that **5** and **7** are dimeric trimethyl monocations, i.e.,  $\{[\text{ArNpy}]_2\text{Zr}_2\text{Me}_3\}[\text{B}(\text{C}_6\text{F}_5)_4]$ . In  $\{[\text{MesN}_2\text{NMe}]_2\text{Zr}_2\text{Me}_3\}^+$  one bridging methyl group ( $J_{\text{CH}} = 133$  Hz), in which  $\text{Zr}-\text{C}-\text{Zr} = 180^\circ$ , and two terminal methyl groups ( $J_{\text{CH}} = 115$  Hz) are present. Since the three methyl groups in **5** and **7** have the same, and relatively low, value for  $J_{\text{CH}}$ , we propose that **5** and **7** contain three bridging methyl groups, as shown in eq 7. The three methyl groups must



scramble intramolecularly, since species of this type are slow to lose  $[\text{ArNpy}]\text{ZrMe}_2$  (see below). Only 0.5 equiv of  $[\text{Ph}_3\text{C}][\text{B}(\text{C}_6\text{F}_5)_4]$  is required to form these dimeric monocations. Therefore the solutions generated by adding 1.0 equiv of activator are dark orange, the color of unreacted  $[\text{Ph}_3\text{C}][\text{B}(\text{C}_6\text{F}_5)_4]$ .

It can be shown readily that the solution obtained upon addition of 1.0 equiv of  $[\text{Ph}_3\text{C}][\text{B}(\text{C}_6\text{F}_5)_4]$  contains 0.5 equiv of unreacted  $[\text{Ph}_3\text{C}][\text{B}(\text{C}_6\text{F}_5)_4]$ . One equivalent of **6** was activated with 1.0 equiv of  $[\text{Ph}_3\text{C}][\text{B}(\text{C}_6\text{F}_5)_4]$  to yield an orange solution whose  $^1\text{H}$  NMR spectrum (20 °C,  $\text{C}_6\text{D}_5\text{Br}$ ) showed resonances for  $\{[\text{TripNpy}]_2\text{Zr}_2\text{Me}_3\}[\text{B}(\text{C}_6\text{F}_5)_4]$  (**7**) and  $\text{Ph}_3\text{CMe}$ . One equivalent of  $^{13}\text{C}$ -labeled **6\*** was then added. The  $^1\text{H}$  NMR spectrum of this solution showed resonances for  $\text{Ph}_3\text{CMe}$  and  $\text{Ph}_3\text{C}^{13}\text{Me}$  in approximately a 1:1 ratio, while the  $^{13}\text{C}\{^1\text{H}\}$  NMR spectrum showed resonances for  $\text{Ph}_3\text{C}^{13}\text{Me}$  and **7\***.

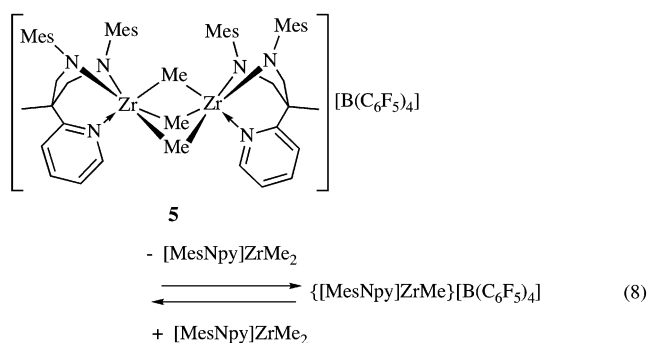
If 0.5 equiv of  $[\text{Ph}_3\text{C}][\text{B}(\text{C}_6\text{F}_5)_4]$  is added to  $[\text{ArNpy}]\text{ZrMe}_2$  complexes, then pale yellow solutions result, since little or no excess trityl is present.  $[\text{TripNpy}]\text{Zr}^{13}\text{Me}_2$  (**6\***) was activated with 0.5 equiv of  $[\text{Ph}_3\text{C}][\text{B}(\text{C}_6\text{F}_5)_4]$  to generate  $\{[\text{TripNpy}]_2\text{Zr}_2^{13}\text{Me}_3\}[\text{B}(\text{C}_6\text{F}_5)_4]$  (**7\***). Variable-temperature  $^{13}\text{C}\{^1\text{H}\}$  studies of this yellow solution in a 1:1 mixture of  $\text{C}_6\text{D}_5\text{Br}$  and  $\text{C}_6\text{D}_5\text{CD}_3$  are essentially identical to those of **6** activated with 1.0 equiv of  $[\text{Ph}_3\text{C}][\text{B}(\text{C}_6\text{F}_5)_4]$ .

(35) Schrock, R. R.; Casado, A. L.; Goodman, J. T.; Liang, L.-C.; Bonitatebus, P. J., Jr.; Davis, W. M. *Organometallics* **2000**, *19*, 5325.



NMR spectra ( $^{13}\text{C}\{^1\text{H}\}$ ) studies in 1:1  $\text{C}_6\text{D}_5\text{Br}:\text{C}_6\text{D}_5\text{CD}_3$  of a mixture of **7\*** and **5** showed no evidence for partially  $^{13}\text{C}$ -labeled **5**. Treatment of **5** with excess  $[\text{Ph}_3\text{C}][\text{B}(\text{C}_6\text{F}_5)_4]$  at 25 °C for 2 h also led to no further activation of the cationic dinuclear species. However, heating the sample to 40 °C for a further 2 h led to approximately 10% further activation, as evident by the presence of  $\text{Ph}_3\text{C}^{13}\text{Me}$  resonances in the  $^1\text{H}$  and  $^{13}\text{C}\{^1\text{H}\}$  NMR spectra (40 °C,  $\text{C}_6\text{D}_5\text{Br}$ ). The dinuclear monocations also do not react readily with excess diethyl ether, THF, or DME at room temperature to give  $[\text{ArNpy}]\text{ZrMe}_2$  and solvent adducts,  $\{[\text{ArNpy}]\text{ZrMeS}_x\}[\text{B}(\text{C}_6\text{F}_5)_4]$ . All of these observations suggest that the dinuclear monocations are relatively stable toward dissociation to give  $\{[\text{ArNpy}]\text{ZrMe}\}[\text{B}(\text{C}_6\text{F}_5)_4]$  and  $[\text{ArNpy}]\text{ZrMe}_2$ . Compounds **5**, **5\***, **7**, and **7\*** were all prepared and isolated as yellow powders. They were all characterized by elemental analysis, as well as by  $^1\text{H}$  and  $^{13}\text{C}\{^1\text{H}\}$  NMR spectroscopy, and had spectra identical to their counterparts generated in situ.

Treatment of  $\{[\text{MesNpy}]_2\text{Zr}_2\text{Me}_3\}[\text{B}(\text{C}_6\text{F}_5)_4]$  (**5**) with 2 equiv of  $[\text{TripNpy}]\text{Zr}(\text{CH}_3)_2$  (**6**) led to a slow exchange of methyl groups between these two species over a period of 4 h at 25 °C, according to  $^{13}\text{C}$  NMR studies. The most plausible mechanism of methyl exchange is for **5** to dissociate as shown in eq 8 to yield  $\{[\text{MesNpy}]\text{ZrMe}\}[\text{B}(\text{C}_6\text{F}_5)_4]$  and  $[\text{MesNpy}]\text{ZrMe}_2$ . At room temper-



ature this equilibrium lies far toward **5**, and virtually no  $\{[\text{MesNpy}]\text{ZrMe}\}[\text{B}(\text{C}_6\text{F}_5)_4]$  is available in solution. However at 40 °C, the rate of forming  $\{[\text{MesNpy}]\text{ZrMe}\}[\text{B}(\text{C}_6\text{F}_5)_4]$  and  $[\text{MesNpy}]\text{ZrMe}_2$  is large enough to result in methyl group exchange between  $\{[\text{MesNpy}]\text{ZrMe}\}[\text{B}(\text{C}_6\text{F}_5)_4]$  and  $[\text{TripNpy}]\text{ZrMe}_2$  or between  $[\text{TripNpy}]\text{ZrMe}_2$  and  $[\text{MesNpy}]\text{ZrMe}_2$ ,<sup>25</sup> or both.

Addition of a large excess of 1-hexene to a solution of isolated  $\{[\text{MesNpy}]_2\text{Zr}_2\text{Me}_3\}[\text{B}(\text{C}_6\text{F}_5)_4]$  in chlorobenzene yielded no poly(1-hexene) over a period of 24 h at 25 °C. Since the exchange described immediately above involves loss of  $[\text{MesNpy}]\text{ZrMe}_2$  from  $\{[\text{MesNpy}]_2\text{Zr}_2\text{Me}_3\}[\text{B}(\text{C}_6\text{F}_5)_4]$  and generation of some  $[\text{MesNpy}]\text{ZrMe}\}[\text{B}(\text{C}_6\text{F}_5)_4]$ , we suspect that the rate of reaction between 1-hexene and  $\{[\text{MesNpy}]\text{ZrMe}\}[\text{B}(\text{C}_6\text{F}_5)_4]$  under the conditions employed simply does not compete with the back reaction between  $[\text{MesNpy}]\text{ZrMe}_2$  and  $\{[\text{MesNpy}]\text{ZrMe}\}[\text{B}(\text{C}_6\text{F}_5)_4]$ . In contrast, the rate of the reaction between  $\{[\text{MesNpy}]\text{ZrMe}\}[\text{B}(\text{C}_6\text{F}_5)_4]$  and  $[\text{TripNpy}]\text{ZrMe}_2$  would be comparable to the rate of the reaction between  $\{[\text{MesNpy}]\text{ZrMe}\}[\text{B}(\text{C}_6\text{F}_5)_4]$  and  $[\text{MesNpy}]\text{ZrMe}_2$ . Therefore slow methyl group exchange is observed.

In view of the above results concerning the formation of dimeric monocations that are inactive for polymeri-

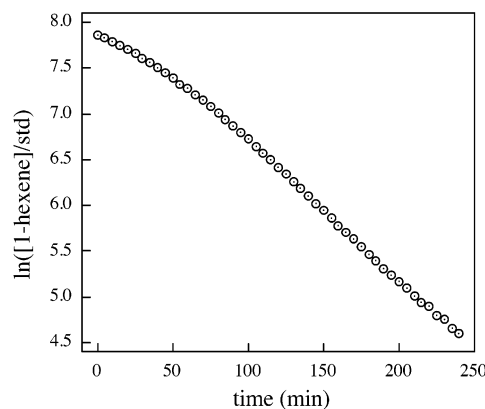


**Figure 8.** Plot of  $\ln[1\text{-hexene}/\text{Ph}_2\text{CH}_2]$  vs time (min) for addition of 160 equiv of 1-hexene to  $[\text{MesNpy}]\text{ZrMe}_2$  (0.007 M) activated with 1 equiv of  $[\text{Ph}_3\text{C}][\text{B}(\text{C}_6\text{F}_5)_4]$  (25 °C,  $\text{C}_6\text{D}_5\text{-Br}$ ).

zation of 1-hexene, we were surprised to find that activation of  $[\text{MesNpy}]\text{ZrMe}_2$  with 1 equiv of  $[\text{Ph}_3\text{C}][\text{B}(\text{C}_6\text{F}_5)_4]$  in chlorobenzene at room temperature followed by addition of 1-hexene does lead to formation of poly(1-hexene), but slowly at room temperature. In a series of carefully controlled polymerizations,  $[\text{MesNpy}]\text{ZrMe}_2$  was activated with 1 equiv of  $[\text{Ph}_3\text{C}][\text{B}(\text{C}_6\text{F}_5)_4]$  in bromobenzene- $d_5$  at -30 °C, and the rates of consumption of up to 200 equiv 1-hexene at 25 °C were determined by monitoring the decrease in 1-hexene concentration with respect to an internal standard using  $^1\text{H}$  NMR spectroscopy. (A control experiment showed that 1-hexene was not polymerized by  $[\text{Ph}_3\text{C}][\text{B}(\text{C}_6\text{F}_5)_4]$  in the absence of zirconium, as expected.) An example is shown in Figure 8. The plot is slightly convex for the first 100 min, but becomes essentially linear thereafter. We propose that under the initiation conditions some  $\{[\text{MesNpy}]\text{ZrMe}\}[\text{B}(\text{C}_6\text{F}_5)_4]$  escapes being captured by  $[\text{MesNpy}]\text{ZrMe}_2$  and therefore is available to act as an initiator for polymerization. The nonlinearity in the early part of the plot can be attributed to a slow initiation process that is able to compete with chain growth in the early stages of polymerization, or perhaps simply to completion of the initiation process. (The 1-hexene was added at low temperature, where the reaction between  $[\text{Ph}_3\text{C}][\text{B}(\text{C}_6\text{F}_5)_4]$  and  $[\text{MesNpy}]\text{ZrMe}_2$  may not have been complete before the sample was warmed to 25 °C.) If we assume that the linear portion of the plot is an approximate measure of the rate constant for polymerization at 25 °C, then  $k_{\text{obs}} = 2.7(2) \times 10^{-4} \text{ s}^{-1}$  at 25 °C.  $^1\text{H}$  and  $^{13}\text{C}$  NMR spectra (25 °C,  $\text{C}_6\text{D}_5\text{Br}$ ) indicate that after all the olefin is consumed, most, if not all, of the initial  $\{[\text{MesNpy}]_2\text{Zr}_2\text{Me}_3\}[\text{B}(\text{C}_6\text{F}_5)_4]$  remains in solution. In another experiment 80 equiv of 1-hexene were added to a sample of catalyst ( $[\text{Zr}]_0 = 0.01 \text{ M}$ ) and the consumption of olefin was monitored at 25 °C. After all the olefin was consumed, a further 80 equiv of 1-hexene were added to the solution and the polymerization process was again monitored. The observed rate constant ( $k_{\text{obs}}$ ) values were  $2.7(2) \times 10^{-4}$  and  $3.0(2) \times 10^{-4} \text{ s}^{-1}$  for the first and second additions, respectively, and little or no  $\{[\text{MesNpy}]_2\text{Zr}_2\text{Me}_3\}[\text{B}(\text{C}_6\text{F}_5)_4]$  appeared to be consumed. No significant initiation period was observed for the second addition. If we calculate the theoretical rate of polymerization of 1-hexene at 25 °C using the activation

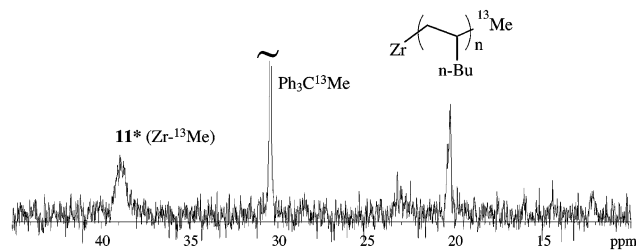


**Figure 9.**  $^{13}\text{C}\{^1\text{H}\}$  NMR spectrum (20 °C,  $\text{C}_6\text{D}_5\text{Br}$ ,  $\text{CH}_3$  resonances) of  $[\text{MesNpy}]\text{Zr}^{13}\text{Me}_2$  activated with 1 equiv of  $[\text{Ph}_3\text{C}][\text{B}(\text{C}_6\text{F}_5)_4]$  after addition of 2 equiv of 1-hexene.

parameters that we found when  $\{[\text{MesNpy}]\text{Zr}(\text{isobutyl})\}-[\text{B}(\text{C}_6\text{F}_5)_4]$  was employed as the initiator, we obtain a theoretical  $k_p = 0.337 \text{ M}^{-1} \text{ s}^{-1}$  or  $k_{\text{obs}} = 3.30 \times 10^{-3} \text{ s}^{-1}$  (at  $[\text{Zr}] = 0.01 \text{ M}$ ), which is  $\sim 10$  times what is observed. Therefore only  $\sim 10\%$  of the zirconium in the activated dimethyl system actually is active for polymerization. It is likely that the amount of  $\{[\text{MesNpy}]\text{ZrMe}\}-[\text{B}(\text{C}_6\text{F}_5)_4]$  that ends up in solution and that therefore is available for initiating polymerization will vary with the temperature of initiation and other slight procedural differences between various experiments.

It was possible to observe the insertion of 1-hexene into the  $\text{Zr}-\text{CH}_3$  bond of the monomeric monocation by treating a solution of  $[\text{MesNpy}]\text{Zr}^{13}\text{Me}_2$  ( $5^*$ , 0.01 M) with 1 equiv of  $[\text{Ph}_3\text{C}][\text{B}(\text{C}_6\text{F}_5)_4]$  followed by 2 equiv of 1-hexene. Although no appreciable amount of polymer was evident after 90 min (because of the low concentration of 1-hexene in this experiment), after 24 h resonances for poly(1-hexene) were observed in the  $^1\text{H}$  NMR spectrum. The  $^{13}\text{C}\{^1\text{H}\}$  NMR spectrum also showed a resonance at 21 ppm as a result of multiple insertion products,<sup>36</sup> as well as peaks corresponding to the unreacted cation and the byproduct,  $\text{Ph}_3\text{CMe}$  (Figure 9). The intensity of the resonance at 21 ppm relative to that ascribed to  $\{[\text{MesNpy}]_2\text{Zr}_2^{13}\text{Me}_3\}[\text{B}(\text{C}_6\text{F}_5)_4]$  at 39 ppm should approximately represent the amount of  $\{[\text{MesNpy}]\text{Zr}^{13}\text{Me}\}\{\text{B}(\text{C}_6\text{F}_5)_4\}$  that has escaped being captured to give  $\{[\text{MesNpy}]_2\text{Zr}_2^{13}\text{Me}_3\}[\text{B}(\text{C}_6\text{F}_5)_4]$  and that therefore is available to initiate polymerization. Although these resonances cannot be integrated accurately under the circumstances, we can at least say that only a fraction of the  $^{13}\text{C}$  originally added to the system turns up in the polymer in this experiment, consistent with our earlier assertion. The quality of this spectrum does not allow us to exclude the possibility of some initial 2,1 insertion into the  $\text{Zr}-\text{Me}$  bond followed by further 1,2 insertions or 2,1 insertion in the propagating species followed by further 1,2 insertions, i.e., enchainment of the regioerror. However, we show below that a 2,1 misinsertion into the initial  $\text{Zr}-\text{Me}$  bond probably results exclusively in  $\beta$ -elimination.

Activation of  $[\text{MesNpy}]\text{ZrMe}_2$  (0.019 M) with 0.5 equiv of  $[\text{Ph}_3\text{C}][\text{B}(\text{C}_6\text{F}_5)_4]$  followed by addition of 43 equiv of 1-hexene led to formation of poly(1-hexene) slowly. The  $\ln[1\text{-hexene}]$  versus time plot is similar to that shown in Figure 8, but the reaction was clearly much slower with  $k_{\text{obs}} = 5.8(2) \times 10^{-5} \text{ s}^{-1}$ , which is one-fifth the value shown in Figure 8. Therefore only  $\sim 2\%$  of the zirconium added to the system is active in this experiment. Not

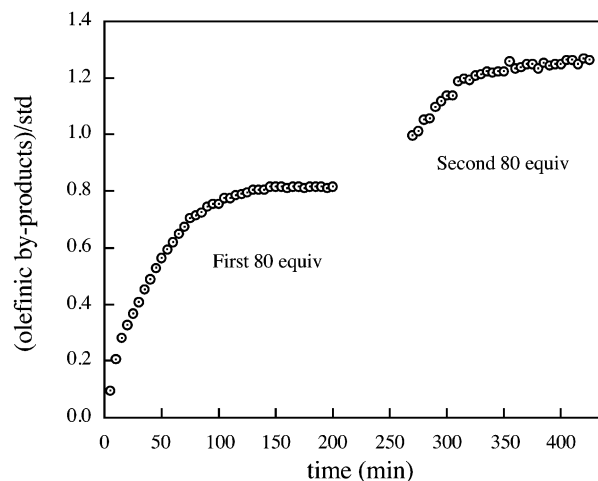


**Figure 10.** Plot of  $[\text{olefinic byproducts}]/\text{C}_6\text{Me}_6$  vs time (min) for two consecutive additions of 80 equiv of 1-hexene to  $[\text{MesNpy}]\text{ZrMe}_2$  (0.01 M) activated with 1 equiv of  $[\text{Ph}_3\text{C}][\text{B}(\text{C}_6\text{F}_5)_4]$  (25 °C,  $\text{C}_6\text{D}_5\text{Br}$ ).

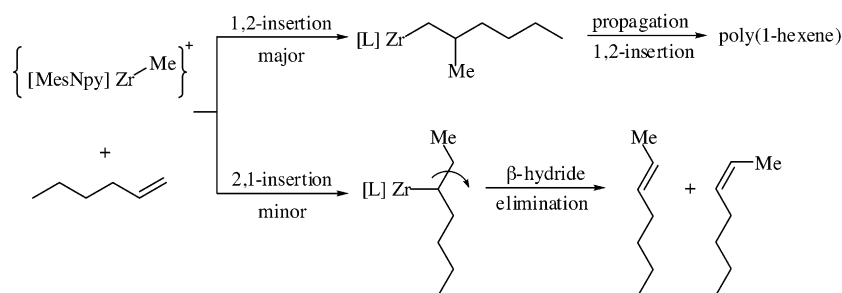
all of the olefin was consumed even after 24 h at room temperature, possibly due to catalyst decomposition by  $\beta$ -hydride elimination under these conditions. Activation of  $[\text{MesNpy}]\text{ZrMe}_2$  (0.0213 M in  $\text{C}_6\text{D}_5\text{Br}$ ) with 0.4 equiv of  $[\text{Ph}_3\text{C}][\text{B}(\text{C}_6\text{F}_5)_4]$  led to a solution that was virtually inactive as a catalyst for the polymerization of 1-hexene (34 equiv in 24 h at 22 °C).

Bulk polymerization results obtained for this system support the assertion that only a small fraction of metal centers catalyze polymerization. Polymer samples obtained from a solution of  $[\text{MesNpy}]\text{ZrMe}_2$  activated with 1.0 equiv of  $[\text{Ph}_3\text{C}][\text{B}(\text{C}_6\text{F}_5)_4]$  at 25 °C have  $M_n$  values that are  $\sim 10$  times greater than expected (Table 2). These data again indicate that only  $\sim 10\%$  of the catalyst is active for polymerization, in agreement with other estimates. In view of the possible complications in the polymerization process at 25 °C ( $\beta$ -hydride elimination and 2,1 insertion into the initial  $\text{Zr}-\text{Me}$  bond; see below), it is surprising that the PDI values are so low. PDI values of this low magnitude in the literature are often said to be “proof” that a polymerization is “living”.

**2,1 Insertion of 1-Hexene into  $\{[\text{MesNpy}]\text{ZrMe}\}-[\text{B}(\text{C}_6\text{F}_5)_4]$ .** In the early stages of polymerization in the activated  $[\text{MesNpy}]\text{ZrMe}_2$  system, two sets of weak resonances appear in the olefinic region of the  $^1\text{H}$  NMR spectra between 5.3 and 5.5 ppm. These resonances are in the region characteristic of internal olefins, which would be formed by  $\beta$ -hydride elimination after a 2,1 insertion.<sup>33,34</sup> The rate of formation of these byproducts (monitored versus a  $\text{C}_6\text{Me}_6$  internal standard) is greatest at the early stages of the polymerization period (Figure 10), and no increase in the  $\beta$ -elimination products was observed after the 1-hexene was fully consumed. A similar pattern (initial increase, then eventual cessation as 1-hexene was consumed) was observed upon addition of another 80 equiv of 1-hexene (Figure 10); the amount formed in the second stage is less than in the first stage. Clearly formation of these products is hexene dependent.

The  $^1\text{H}$  NMR spectra of reaction mixtures that contain these internal olefin byproducts show a splitting pattern that is superimposable on the pattern of a 4:1 mixture

(36) Baumann, R.; Schrock, R. R. *J. Organomet. Chem.* **1998**, *557*, 69.

Scheme 1. Proposed Origin of 2-Heptenes<sup>a</sup>

<sup>a</sup> L = [MesNpy]<sup>2-</sup>, anion = [B(C<sub>6</sub>F<sub>5</sub>)<sub>4</sub>]<sup>-</sup>.

of *trans*-2-heptene and *cis*-2-heptene, as shown in Figure 11. Therefore it would appear that these olefins form via 2,1 insertion of 1-hexene into the Zr–CH<sub>3</sub> bond in {[MesNpy]ZrMe}[B(C<sub>6</sub>F<sub>5</sub>)<sub>4</sub>], as shown in Scheme 1, followed by β-elimination. 3-Heptenes do not form, perhaps because of the more facile β-hydride elimination in the ethyl group versus the butyl group in the internal alkyl. No β-hydride elimination products of this type were observed when {[MesNpy]Zr(isobutyl)}[B(C<sub>6</sub>F<sub>5</sub>)<sub>4</sub>] was employed as the initiator at 0 °C. Therefore the 2,1 regioerror in {[MesNpy]ZrMe}[B(C<sub>6</sub>F<sub>5</sub>)<sub>4</sub>] at 25 °C can be ascribed to differences (largely steric) between insertion into a methyl group (at 25 °C) versus that into an isobutyl group (at 0 °C).

Integration versus a C<sub>6</sub>Me<sub>6</sub> internal standard reveals that the amount of olefin present after addition of 160 equiv of 1-hexene is ~4% of the total metal added to the system. This integration is relatively inaccurate because of the small quantities. We also know that the amount of {[MesNpy]ZrMe}[B(C<sub>6</sub>F<sub>5</sub>)<sub>4</sub>] initiator present in solution initially is only 10–15% of the total metal that has been added. Therefore a “misinsertion” into the initial Zr–Me bond followed by β-hydride elimination could take place approximately one-third of the time (at room temperature). We are proposing that no 2,1 misinsertion product is enchainned and that each 2,1 insertion error is followed by β-hydride elimination. We do *not* know whether the metal-containing product of β-hydride elimination reacts with 1-hexene or decom-

poses too quickly to do so. Nevertheless, and perhaps surprisingly, bulk polymerization of 1-hexene at room temperature with the Zr–Me initiator results in polymers with low PDI values, even though the Zr–Me initiator is clearly not an ideal living system, to say the least.

**Activation of [MesNpy]HfMe<sub>2</sub> and Labeling Studies.** Activation of [MesNpy]HfMe<sub>2</sub> with 1.0 equiv of [Ph<sub>3</sub>C][B(C<sub>6</sub>F<sub>5</sub>)<sub>4</sub>] consumes only half of the activator and results in formation of the dinuclear complex {[MesNpy]<sub>2</sub>Hf<sub>2</sub>Me<sub>3</sub>}[B(C<sub>6</sub>F<sub>5</sub>)<sub>4</sub>] (eq 9). The <sup>1</sup>H NMR chemical shifts for this species correspond closely to those for {[MesNpy]<sub>2</sub>Zr<sub>2</sub>Me<sub>3</sub>}[B(C<sub>6</sub>F<sub>5</sub>)<sub>4</sub>]. Activation of [MesNpy]HfMe<sub>2</sub> with 0.5 equiv of B(C<sub>6</sub>F<sub>5</sub>)<sub>3</sub> results in methyl abstraction and formation of {[MesNpy]<sub>2</sub>Hf<sub>2</sub>Me<sub>3</sub>}[MeB(C<sub>6</sub>F<sub>5</sub>)<sub>3</sub>]. This species and its <sup>13</sup>CH<sub>3</sub> labeled analogue have been isolated and characterized by proton and carbon NMR spectroscopy (see Experimental Section) and by elemental analysis. In view of the (now not unexpected) fact that addition of 96 equiv of 1-hexene to a solution of isolated {[MesNpy]<sub>2</sub>Hf<sub>2</sub>Me<sub>3</sub>}[B(C<sub>6</sub>F<sub>5</sub>)<sub>4</sub>] (0.009 M in C<sub>6</sub>D<sub>5</sub>Br) resulted in no polymerization in 2 h at 22 °C the hafnium dimeric monocation was not studied further. We have no reason to believe that the hafnium system would differ in any significant way from the zirconium system.

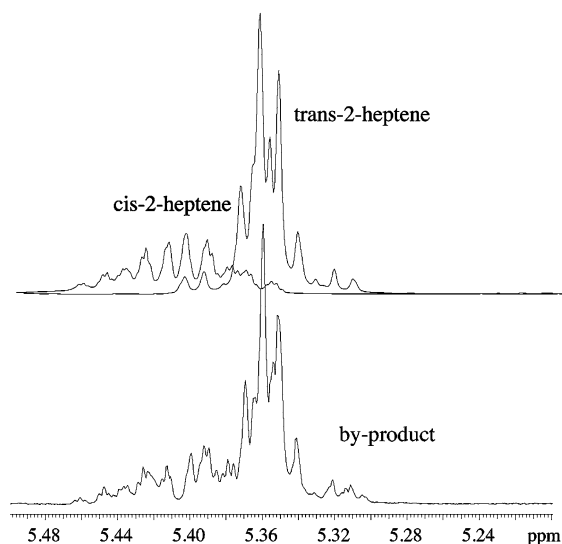
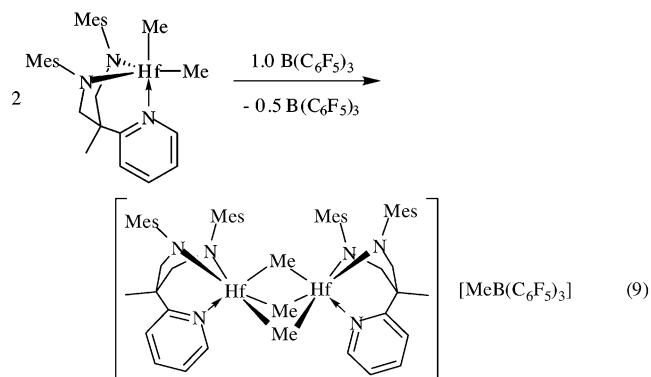


**Figure 11.** Proton NMR spectra of the olefinic byproducts of 1-hexene polymerization by activated [MesNpy]ZrMe<sub>2</sub> compared to a 4:1 mixture of *trans*- and *cis*-2-heptene.



## Discussion

It has become clear that the term “living polymerization” means different things to different people.<sup>37</sup> However, the strict interpretation of “living”, as outlined in a recent review article<sup>1</sup> by Coates, relies on seven criteria. With some changes in wording they are the following: (1) all monomer is consumed, and addition

(37) Darling, T. R.; Davis, T. P.; Fryd, M.; Gridnev, A. A.; Haddleton, D. M.; Ittel, S. D.; Mathieson, R. R., Jr.; Moad, G.; Rizzardo, E. *J. Polym. Sci.: Part A: Polym. Chem.* **2000**, *38*, 1706.

of more monomer leads to further consumption at the same rate; (2)  $M_n$  increases linearly as a function of conversion; (3) the number of active centers remains constant; (4)  $M_n$  can be controlled precisely through stoichiometry; (5) polydispersities are essentially those expected in theory from a perfect living polymerization, i.e., close to 1 (e.g., 1.05) for a polymer of reasonable length (e.g., a 500-mer or larger); (6) block copolymers can be prepared by sequential addition of two different monomers; and (7) the living polymer chain ends can be end-functionalized quantitatively. Of course it is not absolutely necessary that all criteria be fulfilled. For example, the first six might be fulfilled, but an end-functionalizing reagent might not have been found. That would not invalidate the living nature of the reaction. On the basis of what we report here we would suggest that two more criteria could be added to this list: (8) the living propagating species should be observable using some technique (such as NMR methods); and (9) the kinetics of polymerization should be understood and explicable. Again, to some extent these are restatements of other criteria. We believe that at least for the Hf systems reported here, and we should state that this is true so far only for 1-hexene, we feel that seven of these (now) nine criteria have been satisfied.

Dimethyl complexes of group 4 metals have been widely studied since they are usually much more stable than dialkyl complexes in which the alkyl contains one or more  $\beta$ -protons, and they are readily activated in several ways. However, it has been known in metallocene systems for some time that methyl groups can readily bridge between metals.<sup>38–46,47</sup> For example, activation of  $\text{Cp}^*\text{ZrMe}_2$  with an excess of the  $\text{B}[\text{C}_6\text{F}_4(2\text{-C}_6\text{F}_5)]_3$  was found to yield only the dinuclear complex  $\{(\text{Cp}^*\text{ZrMe})_2\text{Me}\}\{\text{MeB}[\text{C}_6\text{F}_4(2\text{-C}_6\text{F}_5)]_3\}$ .<sup>48</sup> This complex has one bridging methyl group with a  $J_{\text{CH}}$  value of  $\sim 130$  Hz, characteristic of  $\text{sp}^2$  hybridization.<sup>48</sup> As stated previously,  $\{[\text{MesN}_2\text{NMe}]_2\text{Zr}_2\text{Me}_3\}[\text{B}(\text{C}_6\text{F}_5)_4]$  ( $[\text{MesN}_2\text{NMe}]^{2-} = [(\text{MesNCH}_2\text{CH}_2)_2\text{NMe}]^{2-}$ ) is formed upon activation of  $[\text{MesN}_2\text{NMe}]\text{ZrMe}_2$  with 0.5 equiv of  $[\text{Ph}_3\text{C}][\text{B}(\text{C}_6\text{F}_5)_4]$ .<sup>35</sup> (The (linear) bridging methyl group in this complex has a  $J_{\text{CH}}$  value of 133 Hz.) However,  $\{[\text{MesN}_2\text{NMe}]_2\text{Zr}_2\text{Me}_3\}[\text{B}(\text{C}_6\text{F}_5)_4]$  dissociates readily into  $\{[\text{MesN}_2\text{NMe}]\text{ZrMe}\}[\text{B}(\text{C}_6\text{F}_5)_4]$  and  $[\text{MesN}_2\text{NMe}]\text{ZrMe}_2$  and therefore reacts further with 0.5 equiv of  $[\text{Ph}_3\text{C}][\text{B}(\text{C}_6\text{F}_5)_4]$  to give a high yield of  $\{[\text{MesN}_2\text{NMe}]\text{ZrMe}\}[\text{B}(\text{C}_6\text{F}_5)_4]$ , the expected product of complete activation. The bimetallic trimethyl monocation is not stable enough to be observed upon activation of  $[\text{t-BuNON}]\text{ZrMe}_2$  ( $[\text{t-BuNON}]^{2-}$

$= [(\text{t-BuN-}o\text{-C}_6\text{H}_4)_2\text{O}]^{2-}$ ) by  $[\text{Ph}_3\text{C}][\text{B}(\text{C}_6\text{F}_5)_4]$  in bromobenzene,<sup>49</sup> presumably because the  $[\text{t-BuNON}]^{2-}$  system is too sterically demanding. The relatively “open” nature of  $\{[\text{MesNpy}]\text{ZrMe}\}^+$  allows a strong adduct with  $[\text{MesNpy}]\text{ZrMe}_2$  to form. The presence of three bridging methyl groups also probably significantly reduces the possibility of losing the  $[\text{MesNpy}]\text{ZrMe}_2$  “base” compared to a complex in which a single bridging methyl group is present.

Reports in the literature have suggested that the alkyl group in the initiator can have a significant effect on the polymerization process. For example, Fink et al. reported that the rate of monomer insertion into a metal–alkyl bond (alkyl  $\neq$  Me) can be up to 100 times faster than insertion into a metal–Me bond.<sup>50–53</sup> (No details of the initiation process were elucidated.) Bochmann et al. have reported that the use of  $\text{Al}(\text{i-Bu})_3$  as a cocatalyst with  $\text{L}_2\text{ZrMe}_2$  systems ( $\text{L}_2 = \text{Cp}_2, \text{rac-Me}_2\text{Si}(\text{Ind})_2$ ) is beneficial as a consequence of alkyl exchange with the cocatalyst to yield  $\text{Zr}(\text{i-Bu})$  species.<sup>54</sup> In this case, the bulkier alkyl group is thought to prevent the formation of catalytically dormant aluminum adducts and thereby increase catalyst efficiency. Marks et al. also have reported significant Zr–alkyl effects on ion pair formation thermodynamics.<sup>55</sup> We have shown here why it is dangerous to draw conclusions about the rate of insertion into various metal–alkyl bonds simply on the basis of the rate of polymerization of a given monomer after what is usually assumed to be complete activation of the dialkyl uncomplicated by side reactions. Nevertheless it is sensible to propose that the rate of insertion into a metal–methyl bond in an initiator is slower than the rate of insertion into the MR bond in a propagating species as a consequence of the anion interacting more strongly with the sterically less demanding  $[\text{MMe}]^+$  system.

The reaction of a terminal olefin with a primary metal alkyl often proceeds largely with 1,2 regiochemistry. Theoretical studies show a clear preference for 1,2 insertion of olefin due to both electronic and steric factors.<sup>56,57</sup> However, regioerrors due to 2,1 insertion of olefin are commonly observed in metallocene systems.<sup>58</sup> In these cases, polymer molecular weights are lowered as chain termination competes with propagation and the hydride product of chain termination reacts with 1-hexene to start another chain.<sup>59</sup> We find that 2,1 insertion into a Zr–Me bond at room temperature is surprisingly facile at 25 °C. Recently, Landis has quantified many of the features of polymerization of 1-hexene by a Zr indenyl system and has found that 2,1 insertion is followed by rapid  $\beta$ -elimination, which gives rise to the

(38) Bochmann, M.; Lancaster, S. J. *Angew. Chem., Int. Ed. Engl.* **1994**, *33*, 1634.

(39) Beck, S.; Prosenč, M. H.; Brintzinger, H. H.; Goretzki, R.; Herfert, N.; Fink, G. *J. Mol. Catal. A* **1996**, *111*, 67.

(40) Koehler, K.; Piers, W. E.; Jarvis, A. P.; Xin, S.; Feng, Y.; Bravakis, A. M.; Collins, S.; Clegg, W.; Yap, G. P. A.; Marder, T. B. *Organometallics* **1998**, *17*, 3557.

(41) Bochmann, M.; Lancaster, S. J.; Hursthouse, M. B.; Malik, K. M. A. *Organometallics* **1994**, *13*, 2235.

(42) Jia, L.; Yang, X.; Stern, C. L.; Marks, T. J. *Organometallics* **1997**, *16*, 842.

(43) Buchwald, S. L.; Lucas, E. A.; Davis, W. M. *J. Am. Chem. Soc.* **1989**, *111*, 397.

(44) Watson, P. L.; Parshall, G. W. *Acc. Chem. Res.* **1985**, *18*, 51.

(45) Watson, P. L. *J. Am. Chem. Soc.* **1983**, *105*, 6491.

(46) Waymouth, R. M.; Santarsiero, B. D.; Grubbs, R. H. *J. Am. Chem. Soc.* **1984**, *106*, 4050.

(47) Chen, E. Y.-X.; Marks, T. J. *Chem. Rev.* **2000**, *100*, 1391.

(48) Chen, E. Y.-X.; Stern, C. L.; Yang, S.; Marks, T. J. *J. Am. Chem. Soc.* **1996**, *118*, 12451.

(49) Goodman, J. T.; Schrock, R. R. *Organometallics* **2001**, *20*, 5205.

(50) Fink, G.; Zoller, W. *Makromol. Chem.* **1981**, *182*, 3265.

(51) Fink, G.; Schnell, D. *Angew. Makromol. Chem.* **1982**, *105*, 31.

(52) Mynott, R.; Fink, G.; W., F. *Angew. Makromol. Chem.* **1987**, *154*, 1.

(53) Fink, G.; Fenzl, W.; Mynott, R. Z. *Naturforsch., B: Chem. Sci.* **1985**, *40b*, 158.

(54) Zhou, J.; Lancaster, S. J.; Walker, D. A.; Beck, S.; Thornton-Pett, M.; Bochmann, M. *J. Am. Chem. Soc.* **2001**, *123*, 223.

(55) Beswick, C. L.; Marks, T. J. *Organometallics* **1999**, *18*, 2410.

(56) Kawamura-Kuribayashi, H.; Koga, N.; Morokuma, K. *J. Am. Chem. Soc.* **1992**, *114*, 8687.

(57) Kawamura-Kuribayashi, H.; Koga, N.; Morokuma, K. *J. Am. Chem. Soc.* **1992**, *114*, 2359.

(58) Resconi, L.; Cavallo, L.; Fait, A.; Piemontesi, F. *Chem. Rev.* **2000**, *100*, 1253.

(59) Resconi, L.; Camurati, I.; Sudmeijer, O. *Top. Catal.* **1999**, *7*, 145.

hexene dependence of  $\beta$ -elimination via 2,1 insertion in that system. Virtually no  $\beta$ -hydride elimination is observed in the hafnium isobutyl systems at 0 °C upon synthesis of up to a 600-mer of poly[1-hexene].

Today it is generally believed that all anions interact to some degree with the cation in a group 4 ionic polymerization system and that, in general, bulky, fluorinated borate anions are some of the more readily accessible weakly coordinating anions.<sup>42,60–63</sup> It also is generally believed that anion effects can be interpreted most readily in terms of the degree of cation/anion “separation”; the more separated and solvated the ion pairs, the more active (but perhaps also the more unstable) the catalyst.<sup>64</sup> We have seen some evidence for well-behaved anion and solvent effects in this work that could be interpreted in this manner. However, we were surprised to find in preliminary experiments that {[MesNpy]Hf(i-Bu)}[HB(C<sub>6</sub>F<sub>5</sub>)<sub>3</sub>] was half as active as {[MesNpy]Hf(i-Bu)}[B(C<sub>6</sub>F<sub>5</sub>)<sub>4</sub>] in bromobenzene. We had expected that a Hf–H–B interaction would dramatically decrease the rate of reaction of an early metal “cation” with an olefin. Apparently that is not the case.

We were surprised to find that hafnium and zirconium complexes polymerize 1-hexene at essentially the same rate. We had expected that the anion would form a tighter ion pair with hafnium and therefore slow the reaction between the ion pair and the olefin. However, the increased strength of the interaction between the olefin and hafnium apparently compensates and the rate overall for hafnium ends up being much the same as for zirconium.

The idea of inhibiting a polymerization reaction catalyzed by a cationic early metal species with an otherwise inert “base” that binds more strongly than an olefin to the metal and thereby limits access of the olefin to the metal is not new. However, we could find no quantitative example of the simple inhibitions that we have demonstrated here, perhaps largely because inhibition is easiest to demonstrate quantitatively in a well-behaved living system. One of the interesting findings is that dimethylaniline may not be a good choice as an inhibitor, although it has been assumed to be innocuous by us<sup>9,49</sup> as well as many other workers in group 4 metal catalyst systems (largely metallocene systems) in the past. Whether CH activation in dimethylaniline takes place in other catalyst systems will depend on the nature of the system, the concentration of catalyst and dimethylaniline, and the monomer being polymerized. For example, ethylene may be polymerized before CH activation can take place, while 1-hexene, for example, may not be. Knowledge of inhibitors in the systems described here ultimately will allow one to choose a protecting group for a given functionalized olefin that would then allow the protected functionalized olefin to be polymerized smoothly.<sup>65</sup>

Rate constants for the polymerization of 1-hexene at 0 °C that we have determined here are listed in Table

**Table 3. Comparison of Several Rate Constants at 0 °C for the Polymerization of 1-Hexene**

compound	solvent	$k_p$ (M <sup>-1</sup> s <sup>-1</sup> )
{[MesNpy]ZrR}[B(C <sub>6</sub> F <sub>5</sub> ) <sub>4</sub> ]	C <sub>6</sub> D <sub>5</sub> Br	0.084
{[t-BuNON]ZrR}[B(C <sub>6</sub> F <sub>5</sub> ) <sub>4</sub> ] <sup>a</sup>	C <sub>6</sub> D <sub>5</sub> Br	0.13
{ <i>rac</i> -[C <sub>2</sub> H <sub>4</sub> (1-indenyl) <sub>2</sub> ]ZrMe}[MeB(C <sub>6</sub> F <sub>5</sub> ) <sub>3</sub> ]	C <sub>6</sub> H <sub>5</sub> CH <sub>3</sub>	2.0
{[MesNpy]HfR}[B(C <sub>6</sub> F <sub>5</sub> ) <sub>4</sub> ]	C <sub>6</sub> D <sub>5</sub> Br	0.10
{[MesNpy]HfR}[HB(C <sub>6</sub> F <sub>5</sub> ) <sub>3</sub> ]	C <sub>6</sub> D <sub>5</sub> Br	0.048
{[MesNpy]HfR}[HB(C <sub>6</sub> F <sub>5</sub> ) <sub>3</sub> ]	C <sub>6</sub> D <sub>5</sub> CD <sub>3</sub>	0.011

<sup>a</sup> [t-BuNON]<sup>2-</sup> = [(t-BuN-*o*-C<sub>6</sub>H<sub>4</sub>)<sub>2</sub>O]<sup>2-</sup> (see refs 36 and 49).

3, along with a value for {[t-BuNON]ZrR}[B(C<sub>6</sub>F<sub>5</sub>)<sub>4</sub>][[t-BuNON]<sup>2-</sup> = [(t-BuN-*o*-C<sub>6</sub>H<sub>4</sub>)<sub>2</sub>O]<sup>2-</sup>]<sup>49</sup> and a recent value obtained by Landis for a nonliving metallocene system.<sup>29,30</sup> The rates for the diamido/donor systems vary by approximately an order of magnitude. However, the metallocene system explored by Landis is ~200 times more active than {[MesNpy]HfR}[HB(C<sub>6</sub>F<sub>5</sub>)<sub>3</sub>] in toluene and ~20 times more active than {[MesNpy]HfR}[B(C<sub>6</sub>F<sub>5</sub>)<sub>4</sub>] in bromobenzene. We ascribe the lower activity of the diamido/donor system in general (compared to a metallocene-based catalyst system) to a delocalization of the metal's positive charge out onto the amido nitrogens. It is also worth noting that the anion may interact more strongly with the cation in the more “open” [MesNpy]<sup>2-</sup> systems than in a metallocenium ion pair and, therefore, may further reduce the electrophilicity of the “cation” and also sterically block the olefin's access to the metal.

In future studies we hope to explore other [MAryl-Npy]<sup>2-</sup> ligand systems (Aryl = triisopropylphenyl<sup>24</sup> or 3,5-dichlorophenyl<sup>66</sup> are known), to explore other types of ligands that appear to give rise to living catalysts, to explore the possibility of polymerizing the appropriately protected functionalized olefin (in which the functionality is remote from the double bond) in a living manner, and to explore the possibility of preparing asymmetric diamido/donor catalysts that will allow isotactic polymers to be prepared in a living manner, a phenomenon that has been reported recently by both Sita<sup>10,12,17</sup> and Kol.<sup>13–15</sup> We also hope to be able to prepare various alkyl cations, even internal alkyl (e.g., isopropyl) cations,<sup>24</sup> study the rate and mechanism of their decomposition, and study the rate at which they react with various olefins. In this manner we hope to address relative stabilities of various alkyls and their reactivities toward olefins directly.

## Experimental Section

**General Procedures.** All manipulations, with the exception of the synthesis of ligand precursors, were performed under N<sub>2</sub> in a glovebox or using standard Schlenk procedures. Solvents were dried using conventional procedures.<sup>67</sup> All catalysts were activated in a glovebox free of ether, THF, and other coordinating solvents. Chlorobenzene (HPLC grade) and deuterated solvents were degassed and stored over and distilled from CaH<sub>2</sub>. Commercial reagents were used without further purification. NMR spectra were recorded on a Varian INOVA 500 spectrometer. <sup>1</sup>H NMR chemical shifts are given in ppm versus residual protons in the deuterated solvents as follows:  $\delta$  7.16 C<sub>6</sub>D<sub>6</sub>,  $\delta$  2.09 toluene-*d*<sub>8</sub> (methyl),  $\delta$  7.29 C<sub>6</sub>D<sub>5</sub>-

(60) Vanka, K.; Chan, M. S. W.; Pye, C. C.; Ziegler, T. *Organometallics* **2000**, *19*, 1841.

(61) Vanka, K.; Ziegler, T. *Organometallics* **2001**, *20*, 905.

(62) Beck, W.; Sunkel, K. *Chem. Rev.* **1988**, *88*, 1405.

(63) Beck, S.; Lieber, S.; Schaper, F.; Geyer, A.; Brintzinger, H.-H. *J. Am. Chem. Soc.* **2001**, *123*, 1483.

(64) Bochmann, M. *Angew. Chem., Int. Ed. Engl.* **1992**, *31*, 1181.

(65) Kesti, M. R.; Coates, G. W.; Waymouth, R. M. *J. Am. Chem. Soc.* **1992**, *114*, 9679.

(66) Araujo, J. P.; Wicht, D. K.; Bonitatebus, P. J. J.; Schrock, R. R. *Organometallics* **2001**, *20*, 5682.

(67) Pangborn, A. B.; Giardello, M. A.; Grubbs, R. H.; Rosen, R. K.; Timmers, F. J. *Organometallics* **1996**, *15*, 1518.

Br (most downfield resonance).  $^{13}\text{C}\{^1\text{H}\}$  NMR chemical shifts are given in ppm versus residual  $^{13}\text{C}$  in the solvents as follows:  $\delta$  128.39  $\text{C}_6\text{D}_6$ ,  $\delta$  20.4 toluene- $d_8$  (methyl),  $\delta$  122.25  $\text{C}_6\text{D}_5\text{Br}$  (most upfield resonance). Inhibitors were dried thoroughly over  $\text{CaH}_2$  and distilled. Dialkyl complexes were prepared as reported in the literature.<sup>25</sup>

GPC analyses were carried out on a system equipped with two Jordi-Gel DVB mixed bed columns (250 mm length  $\times$  10 mm inner diameter) in series. HPLC grade THF was supplied at a flow rate of 1.0 mL/min with a Knauer 64 HPLC pump. A Wyatt Technology mini Dawn light-scattering detector coupled with a Knauer differential refractometer was employed. Data analysis was carried out using Astrette 1.2 software (Wyatt Technology).  $M_n$  and  $M_w$  values for poly(1-hexene) were obtained using  $dn/dc = 0.076$  mL/gr (Wyatt Technology), and the auxiliary constant of the apparatus ( $5.9 \times 10^{-4}$ ) was calibrated using a polystyrene standard ( $M_n = 2.2 \times 10^5$ ).

**Observation of  $\{[\text{MesNpy}]\text{Hf}(\text{i-Bu})\}[\text{B}(\text{C}_6\text{F}_5)_4]$ .** Solutions of  $[\text{MesNpy}]\text{Hf}(\text{i-Bu})_2$  (0.0091 g, 0.013 mmol) and  $[\text{Ph}_3\text{C}][\text{B}(\text{C}_6\text{F}_5)_4]$  (0.0122 g, 0.0132 mmol), each in  $\text{C}_6\text{D}_5\text{Br}$  (0.5 mL), were prepared and cooled to  $-30^\circ\text{C}$ . The solutions were mixed while still cold, and the resulting yellow solution was transferred to an NMR tube and frozen in liquid nitrogen within 2 min of the preparation of the sample.  $^1\text{H}$  NMR (500 MHz,  $\text{C}_6\text{D}_5\text{Br}$ , 273 K):  $\delta$  0.44 (d, 2H, Hf- $\text{CH}_2\text{CH}(\text{CH}_3)_2$ ), 0.55 (d, 3H, Hf- $\text{CH}_2\text{CH}(\text{CH}_3)_2$ ), 1.28 (s, 3H,  $\text{CH}_3$ ), 1.57 (br s, 6H,  $o\text{-CH}_3$ ), 1.62 (s, 6H,  $\text{CH}_2\text{C}(\text{CH}_3)_2$ ), 1.73 (m, 1H, Hf- $\text{CH}_2\text{CH}(\text{CH}_3)_2$ ), 2.18 (s, 6H,  $p\text{-CH}_3$ ), 2.35 (br s, 6H,  $o\text{-CH}_3$ ), 2.95 (d, 2H,  $\text{CH}_2$ ), 4.22 (d, 2H,  $\text{CH}_2$ ), 4.73 (s, 2H,  $\text{CH}_2\text{C}(\text{CH}_3)_2$ ), 5.45 (s, 1H,  $\text{Ph}_3\text{CH}$ ), 6.77 (br s, 2H,  $\text{CH}$ ), 6.85 (br s, 2H,  $\text{CH}$ ), 7.23 (m, 1H,  $py\text{-CH}$ ), 7.38 (m, 1H,  $py\text{-CH}$ ), 7.69 (m, 1H,  $py\text{-CH}$ ), 8.54 (m, 1H,  $py\text{-}o\text{-CH}$ ).  $^{13}\text{C}\{^1\text{H}\}$  NMR (125 MHz,  $\text{C}_6\text{D}_5\text{Br}$ , 273 K):  $\delta$  18.57 (s,  $o\text{-CH}_3$ ), 20.73 (s,  $p\text{-CH}_3$ ), 24.20 (s,  $\text{CH}_2\text{C}(\text{CH}_3)_2$ ), 24.91 (s,  $\text{CH}_3$ ), 27.58 (s, Hf- $\text{CH}_2\text{CH}(\text{CH}_3)_2$ ), 28.75 (s, Hf- $\text{CH}_2\text{CH}(\text{CH}_3)_2$ ), 42.79 (s,  $\text{CR}_4$ ), 56.79 (s,  $\text{Ph}_3\text{CH}$ ), 64.25 (s,  $\text{CH}_2$ ), 93.34 (s, Hf- $\text{CH}_2\text{CH}(\text{CH}_3)_2$ ), 111.23 (s,  $\text{CH}_2\text{C}(\text{CH}_3)_2$ ). Some aryl peaks are omitted from both the proton and the carbon NMR data.

**Reactions of  $\{[\text{MesNpy}]\text{Hf}(\text{i-Bu})\}[\text{B}(\text{C}_6\text{F}_5)_4]$  with 1-Hexene: Kinetic Studies.** Solutions of  $[\text{MesNpy}]\text{Hf}(\text{i-Bu})_2$  (0.0091 g, 0.013 mmol) and  $[\text{Ph}_3\text{C}][\text{B}(\text{C}_6\text{F}_5)_4]$  (0.0122 g, 0.013 mmol), each in  $\text{C}_6\text{D}_5\text{Br}$  (0.5 mL), were prepared and cooled to  $-30^\circ\text{C}$ . The solutions were mixed while still cold, and 1-hexene (0.100 mL, 0.80 mmol) was added to the mixture. The NMR samples were obtained directly from this solution and frozen in liquid nitrogen prior to examination.

Polymerizations of the other olefins listed in Table 1 were carried out similarly.

**Reactions of  $\{[\text{MesNpy}]\text{Hf}(\text{i-Bu})\}[\text{B}(\text{C}_6\text{F}_5)_4]$  with 1-Hexene: Bulk Polymerization.** Solutions of  $[\text{MesNpy}]\text{Hf}(\text{i-Bu})_2$  (0.0131 g, 0.0189 mmol) and  $[\text{Ph}_3\text{C}][\text{B}(\text{C}_6\text{F}_5)_4]$  (0.0177 g, 0.0192 mmol), each in  $\text{C}_6\text{H}_5\text{Cl}$  (1.5 mL), were prepared and cooled to  $-30^\circ\text{C}$ . The solutions were mixed while still cold, and 1-hexene (0.700 mL, 5.60 mmol) was added to the mixture. The samples were stirred at  $0^\circ\text{C}$  for 2 h and quenched with methanol. The solvent was then removed in vacuo and the residue dissolved in pentane. The solution was passed through silica and the pentane removed in vacuo (16 h) at room temperature.

$\{[\text{MesNpy}]\text{Hf}(\text{C}_6\text{H}_4\text{NMe}_2)\}[\text{HB}(\text{C}_6\text{F}_5)_3]$ . Solutions of  $[\text{MesNpy}]\text{Hf}(\text{i-Bu})_2$  (0.324 g, 0.468 mmol) and  $\text{B}(\text{C}_6\text{F}_5)_3$  (0.240 g, 0.468 mmol) in  $\text{C}_6\text{H}_5\text{Cl}$  and toluene, respectively (total volume = 3.0 mL), were prepared and cooled to  $-30^\circ\text{C}$  for 30 min. The solutions were mixed while still cold, and the yellow mixture was stirred at  $0^\circ\text{C}$  for 24 h. The solvent was removed in vacuo, and the residue was triturated with pentane to yield yellow powder; yield 0.410 g (72%).  $^1\text{H}$  NMR (500 MHz,  $\text{C}_6\text{D}_5\text{Br}$ , 293 K):  $\delta$  1.36 (s, 3H,  $\text{CH}_3$ ), 1.50 (s, 6H,  $o\text{-CH}_3$ ), 2.03 (s, 6H,  $p\text{-CH}_3$ ), 2.13 (s, 6H,  $\text{N-CH}_3$ ), 2.32 (s, 6H,  $p\text{-CH}_3$ ), 2.94 (d, 2H,  $\text{CH}_2$ ), 4.42 (d, 2H,  $\text{CH}_2$ ), 6.71 (m, 1H,  $\text{anil-CH}$ ), 6.43 (s, 2H,  $\text{mes-CH}$ ), 6.73 (s, 2H,  $\text{mes-CH}$ ), 6.99 (m, 1H,  $\text{anil-CH}$ ), 7.21 (m, 1H,  $py\text{-CH}$ ), 7.43 (m, 1H,  $py\text{-CH}$ ), 7.47 (m, 1H,  $\text{anil-CH}$ ),

7.83 (m, 1H,  $py\text{-CH}$ ), 7.85 (m, 1H,  $\text{anil-CH}$ ), 9.02 (m, 1H,  $py\text{-}o\text{-CH}$ ).  $^{13}\text{C}\{^1\text{H}\}$  NMR (125 MHz,  $\text{C}_6\text{D}_5\text{Br}$ , 293 K):  $\delta$  18.13 (s,  $o\text{-CH}_3$ ), 19.82 (s,  $o\text{-CH}_3$ ), 20.82 (s,  $p\text{-CH}_3$ ), 22.72 (s,  $\text{CH}_3$ ), 43.17 (s,  $\text{CR}_4$ ), 47.89 (s,  $\text{N-CH}_3$ ), 64.48 (s,  $\text{CH}_2$ ), 99.74 (s,  $\text{Ar-C}$ ), (some aryl peaks omitted here), 186.06 (s,  $\text{Ar-C}$ ). Anal. Calcd for  $\text{C}_{53}\text{H}_{44}\text{N}_4\text{BF}_{15}\text{Hf}$ : C, 52.56; H, 3.66; N, 4.63. Found: C, 52.63; H, 3.61; N, 4.57.

**Inhibition Studies. Polymerization of 1-Hexene with  $\{[\text{MesNpy}]\text{Hf}(\text{i-Bu})\}[\text{B}(\text{C}_6\text{F}_5)_4]$  in the Presence of (i-Pr) $_2\text{O}$ .** Solutions of  $[\text{MesNpy}]\text{Hf}(\text{i-Bu})_2$  (0.0129 g, 0.0186 mmol) and  $[\text{Ph}_3\text{C}][\text{B}(\text{C}_6\text{F}_5)_4]$  (0.0178 g, 0.0193 mmol), each in  $\text{C}_6\text{D}_5\text{Br}$  (0.4 mL), were prepared and cooled to  $-30^\circ\text{C}$ . The solutions were mixed while still cold, and (i-Pr) $_2\text{O}$  (0.015 mL, 0.11 mmol) was added and the mixture was stirred vigorously. 1-Hexene (0.200 mL, 1.60 mmol) was then added to the mixture. The NMR samples were obtained directly from this solution and frozen in liquid nitrogen prior to examination.

Other inhibition studies were carried out similarly.

**Observation of  $\{[\text{MesNpy}]\text{Zr}(\text{i-Bu})\}[\text{B}(\text{C}_6\text{F}_5)_4]$ .** *Note: all of the following manipulations were carried out in the absence of light.* Solutions of  $[\text{MesNpy}]\text{Zr}(\text{i-Bu})_2$  (0.022 g, 0.036 mmol) and  $[\text{Ph}_3\text{C}][\text{B}(\text{C}_6\text{F}_5)_4]$  (0.034 g, 0.036 mmol), each in  $\text{C}_6\text{D}_5\text{Br}$  (0.5 mL), were prepared and cooled to  $-30^\circ\text{C}$ . The solutions were mixed while still cold, and the resulting yellow/orange solution was transferred to an NMR tube and frozen in liquid nitrogen within 2 min of the preparation of the sample.  $^1\text{H}$  NMR (500 MHz,  $\text{C}_6\text{D}_5\text{Br}$ , 243 K):  $\delta$  0.60 (d, 6H, Zr- $\text{CH}_2\text{CH}(\text{CH}_3)_2$ ), 0.62 (d, 2H, Zr- $\text{CH}_2\text{CH}(\text{CH}_3)_2$ ), 0.84 (m, 1H,  $\text{CH}_2\text{-CH}(\text{CH}_3)_2$ ), 1.31 (s, 3H,  $\text{CH}_3$ ),  $\sim 1.5$  (br s, 6H,  $o\text{-CH}_3$ ), 1.62 (s, 6H,  $\text{CH}_2\text{C}(\text{CH}_3)_2$ ), 2.18 (s, 6H,  $p\text{-CH}_3$ ), 2.32 (br s, 6H,  $o\text{-CH}_3$ ), 2.79 (d, 2H,  $\text{CH}_2$ ), 3.98 (d, 2H,  $\text{CH}_2$ ), 4.73 (s, 1H,  $\text{Ph}_3\text{CH}$ ), 5.45 (s, 2H,  $\text{CH}_2\text{C}(\text{CH}_3)_2$ ), some aryl peaks omitted here, 7.36 (m, 1H,  $py\text{-CH}$ ), 7.65 (m, 1H,  $py\text{-CH}$ ), 8.39 (m, 1H,  $py\text{-}o\text{-CH}$ ).  $^{13}\text{C}\{^1\text{H}\}$  NMR (125 MHz,  $\text{C}_6\text{D}_5\text{Br}$ , 243 K):  $\delta$  18.65 (s,  $o\text{-CH}_3$ ), 20.79 (s,  $p\text{-CH}_3$ ), 24.30 (s,  $\text{CH}_2\text{C}(\text{CH}_3)_2$ ), 24.96 (s,  $\text{CH}_3$ ), 26.28 (s, Zr- $\text{CH}_2\text{CH}(\text{CH}_3)_2$ ), 27.533 (s, Zr- $\text{CH}_2\text{CH}(\text{CH}_3)_2$ ), 44.76 (s,  $\text{CR}_4$ ), 56.64 (s,  $\text{Ph}_3\text{CH}$ ), 64.77 (s,  $\text{CH}_2$ ), 83.33 (s, Zr- $\text{CH}_2\text{CH}(\text{CH}_3)_2$ ), 111.23 (s,  $\text{CH}_2\text{C}(\text{CH}_3)_2$ ). (Some aryl peaks are omitted.) The reaction is cleanest when carried out with freshly prepared and recrystallized  $[\text{MesNpy}]\text{Zr}(\text{i-Bu})_2$ .

**Reactions of  $\{[\text{MesNpy}]\text{Zr}(\text{i-Bu})\}[\text{B}(\text{C}_6\text{F}_5)_4]$  with 1-Hexene: Kinetic Studies.** *Note: all of the following manipulations were carried out in the absence of light.* Solutions of  $[\text{MesNpy}]\text{Zr}(\text{i-Bu})_2$  (0.0082 g, 0.0136 mmol) and  $[\text{Ph}_3\text{C}][\text{B}(\text{C}_6\text{F}_5)_4]$  (0.0136 g, 0.0147 mmol), each in  $\text{C}_6\text{D}_5\text{Br}$  (0.8 mL), were prepared and cooled to  $-30^\circ\text{C}$ . The solutions were mixed while still cold, and 1-hexene (0.170 mL, 1.36 mmol) was added to the mixture. The total volume was increased to 2 mL in a volumetric flask. The NMR samples were obtained directly from this solution and frozen with liquid nitrogen prior to experimentation. The reaction is most reproducible when carried out with freshly prepared and recrystallized  $[\text{MesNpy}]\text{Zr}(\text{i-Bu})_2$ . In two cases (107 and 220 equiv of 1-hexene with  $[\text{Zr}] = 15$  and 7.3 mM, respectively) the samples were quenched with methanol after polymerization was complete, and the solvent was removed in vacuo. The polymer sample was then redissolved in pentane, the solution was passed through silica, and the pentane was removed in vacuo (16 h).

**Reactions of Activated  $[\text{MesNpy}]\text{ZrMe}_2$  with 1-Hexene: Kinetic Studies.** Solutions of  $[\text{MesNpy}]\text{ZrMe}_2$  (0.0298 g, 0.0572 mmol) and  $[\text{Ph}_3\text{C}][\text{B}(\text{C}_6\text{F}_5)_4]$  (0.0535 g, 0.0580 mmol), each in  $\text{C}_6\text{D}_5\text{Br}$  (2 mL), were prepared and cooled to  $-30^\circ\text{C}$ . The solutions were mixed while still cold, and hexamethylbenzene (HMB) (0.0582, 0.0359 mmol) was added to the resulting orange solution. The total volume was increased to 5 mL in a volumetric flask, and the solution was stored at  $-30^\circ\text{C}$  for further use for up to 5 days.  $^{13}\text{C}$  labeling studies were carried out in a similar fashion using  $[\text{MesNpy}]\text{Zr}^{13}\text{Me}_2$ .

The NMR samples were prepared by adding 1-hexene (0.100 mL, 0.800 mmol) to the above stock solution (0.900 mL, 0.0099 mmol) in a calibrated NMR tube.  $^1\text{H}$  NMR (500 MHz,  $\text{C}_6\text{D}_5\text{Br}$ ,

Br) spectra were obtained by comparison of the most downfield methylene peak of 1-hexene  $\delta$  1.96 (m, 2H,  $\text{CH}_2=\text{CHCH}_2(\text{CH}_2)_2\text{-CH}_3$ ) to the hexamethylbenzene peak 2.10 (s, 18H,  $\text{CH}_3$ ).

**Activation of [MesNpy]ZrMe<sub>2</sub> with [Ph<sub>3</sub>C][B(C<sub>6</sub>F<sub>5</sub>)<sub>4</sub>].** Solutions of [MesNpy]ZrMe<sub>2</sub> (0.021 g, 0.040 mmol) and [Ph<sub>3</sub>C][B(C<sub>6</sub>F<sub>5</sub>)<sub>4</sub>] (0.037 g, 0.040 mmol), each in C<sub>6</sub>D<sub>5</sub>Br (0.6 mL), were prepared and cooled to  $-30^\circ\text{C}$ . The solutions were mixed while still cold, and the resulting orange solution was transferred to an NMR tube. The following NMR data correspond to activated [MesNpy]Zr(<sup>13</sup>Me)<sub>2</sub>, which was obtained in an analogous process. <sup>1</sup>H NMR (500 MHz, C<sub>6</sub>D<sub>5</sub>Br, 295 K):  $\delta$  0.66 (d,  $J_{\text{CH}} = 108$  Hz, 3H, Zr-<sup>13</sup>CH<sub>3</sub>), 1.21 (s, 3H, CH<sub>3</sub>), 1.22 (s, 6H, *o*-CH<sub>3</sub>), 2.03 (d,  $J_{\text{CH}} = 128$  Hz, 3H, <sup>13</sup>CH<sub>3</sub>Ph<sub>3</sub>), 2.15 (s, 6H, *p*-CH<sub>3</sub>), 2.29 (s, 6H, *o*-CH<sub>3</sub>), 2.78 (d, 2H, CH<sub>2</sub>), 3.67 (d, 2H, CH<sub>2</sub>), 6.70 (s, 2H, CH), 6.80 (s, 2H, CH), some aryl peaks omitted here, 6.87 (m, 1H, py-CH), 7.51 (m, 1H, py-CH), 7.92 (m, 1H, py-*o*-CH). <sup>13</sup>C{<sup>1</sup>H} NMR (125 MHz, C<sub>6</sub>D<sub>5</sub>Br, 295 K):  $\delta$  17.14 (s, *o*-CH<sub>3</sub>), 18.10 (s, *o*-CH<sub>3</sub>), 20.80 (s, *p*-CH<sub>3</sub>), 23.81 (s, CH<sub>3</sub>), 30.42 (s, <sup>13</sup>CH<sub>3</sub>Ph<sub>3</sub>), 38.81 (br s, Zr-<sup>13</sup>CH<sub>3</sub>), 48.95 (s, CR<sub>4</sub>), 67.40 (s, CH<sub>2</sub>) (Some aryl resonances are omitted.)

**Isolation of {[MesNpy]<sub>2</sub>Zr<sub>2</sub>Me<sub>3</sub>}[B(C<sub>6</sub>F<sub>5</sub>)<sub>4</sub>].** Solutions of [MesNpy]ZrMe<sub>2</sub> (0.205 g, 0.394 mmol) and [Ph<sub>3</sub>C][B(C<sub>6</sub>F<sub>5</sub>)<sub>4</sub>] (0.182 g, 0.197 mmol), each in C<sub>6</sub>H<sub>5</sub>Cl (1.5 mL), were prepared and cooled to  $-30^\circ\text{C}$ . The solutions were mixed while still cold, and the resulting yellow solution was stirred at room temperature for 5 min. The solvent was removed in vacuo and the remaining residue triturated with pentane for 2 h. The resulting yellow powder was washed with pentane to remove Ph<sub>3</sub>CMe and dried in vacuo; yield 0.233 g (64%). The <sup>13</sup>C-labeled analogue was prepared in a similar fashion from [MesNpy]Zr(<sup>13</sup>Me)<sub>2</sub>. <sup>1</sup>H NMR (500 MHz, C<sub>6</sub>D<sub>6</sub>, 295 K):  $\delta$  0.74 (s, 4.5 H, Zr-CH<sub>3</sub>), 0.86 (s, 3H, CH<sub>3</sub>), 1.22 (s, 6H, *o*-CH<sub>3</sub>), 2.14 (s, 6H, *p*-CH<sub>3</sub>), 2.27 (s, 6H, *o*-CH<sub>3</sub>), 2.65 (d, 2H, CH<sub>2</sub>), 3.67 (d, 2H, CH<sub>2</sub>), 6.67 (m, 1H, py-CH), 6.73 (s, 2H, CH), 6.78 (s, 2H, CH), 6.88 (m, 1H, py-CH), 7.18 (m, 1H, py-CH), 7.99 (m, 1H, py-*o*-CH). <sup>1</sup>H NMR (500 MHz, C<sub>6</sub>D<sub>5</sub>Br, 295 K):  $\delta$  0.66 (d,  $J_{\text{CH}} = 108$  Hz, H, Zr-<sup>13</sup>CH<sub>3</sub>), 1.21 (s, 3H, CH<sub>3</sub>), 1.22 (s, 6H, *o*-CH<sub>3</sub>), 2.15 (s, 6H, *p*-CH<sub>3</sub>), 2.29 (s, 6H, *o*-CH<sub>3</sub>), 2.78 (d, 2H, CH<sub>2</sub>), 3.67 (d, 2H, CH<sub>2</sub>), 6.70 (s, 2H, CH), 6.80 (s, 2H, CH), 6.87 (m, 1H, py-CH), 7.25 (m, 1H, py-CH), 7.51 (m, 1H, py-CH), 7.92 (m, 1H, py-*o*-CH). Anal. Calcd for C<sub>93</sub>H<sub>75</sub>N<sub>6</sub>Zr<sub>2</sub>BF<sub>20</sub>: C, 60.38; H, 4.09; N, 4.54. Found: C, 60.46; H, 4.19; N, 4.59.

**Activation of [TripNpy]ZrMe<sub>2</sub> with [Ph<sub>3</sub>C][B(C<sub>6</sub>F<sub>5</sub>)<sub>4</sub>].** Solutions of [TripNpy]ZrMe<sub>2</sub> (0.0102 g, 0.0148 mmol) and [Ph<sub>3</sub>C][B(C<sub>6</sub>F<sub>5</sub>)<sub>4</sub>] (0.0139 g, 0.0151 mmol), each in C<sub>6</sub>D<sub>5</sub>Br (0.5 mL), were prepared and cooled to  $-30^\circ\text{C}$ . The solutions were mixed while still cold, and the resulting orange solution was transferred to an NMR tube.

**{[TripNpy]<sub>2</sub>Zr<sub>2</sub>Me<sub>3</sub>}[B(C<sub>6</sub>F<sub>5</sub>)<sub>4</sub>].** Solutions of [TripNpy]ZrMe<sub>2</sub> (0.290 g, 0.421 mmol) and [Ph<sub>3</sub>C][B(C<sub>6</sub>F<sub>5</sub>)<sub>4</sub>] (0.194 g, 0.210 mmol), each in C<sub>6</sub>H<sub>5</sub>Cl (1.5 mL), were prepared and cooled to  $-30^\circ\text{C}$ . The solutions were mixed while still cold,

and the resulting yellow solution was stirred at room temperature for 5 min. The solvent was removed in vacuo and remaining residue triturated with pentane for 2 h. The resulting yellow powder was washed with pentane to remove Ph<sub>3</sub>CMe and dried in vacuo; yield 0.320 g (75%). {[TripNpy]<sub>2</sub>Zr<sub>2</sub>(<sup>13</sup>Me<sub>3</sub>)[B(C<sub>6</sub>F<sub>5</sub>)<sub>4</sub>] was prepared in a similar fashion from [TripNpy]Zr(<sup>13</sup>Me)<sub>2</sub>. <sup>1</sup>H NMR (500 MHz, C<sub>6</sub>D<sub>6</sub>, 295 K):  $\delta$  0.64 (d, 6H, CH<sub>3</sub>), 0.81 (d, 6H, CH<sub>3</sub>), 0.89 (s, 3H, CH<sub>3</sub>), 1.02 (s, 4.5H, Zr-CH<sub>3</sub>), 1.05 (d, 6H, CH<sub>3</sub>), 1.26 (d, 6H, CH<sub>3</sub>), 1.33 (d, 12H, CH<sub>3</sub>), 1.67 (m, 2H, CH), 2.83 (m, 2H, CH), 3.00 (d, 2H, CH<sub>2</sub>), 3.56 (m, 2H, CH), 3.73 (d, 2H, CH<sub>2</sub>), 6.84 (m, 1H, py-CH), 6.85 (s, 2H, CH), 6.91 (m, 1H, py-CH), 6.93 (s, 2H, CH), 7.39 (m, 1H, py-CH), 8.59 (m, 1H, py-*o*-CH). Anal. Calcd for C<sub>105</sub>H<sub>123</sub>N<sub>6</sub>Zr<sub>2</sub>BF<sub>20</sub>: C, 61.75; H, 6.07; N, 4.11. Found: C, 61.64; H, 6.18; N, 3.98.

**Activation of [MesNpy]HfMe<sub>2</sub> with [Ph<sub>3</sub>C][B(C<sub>6</sub>F<sub>5</sub>)<sub>4</sub>].** Solutions of [MesNpy]HfMe<sub>2</sub> (0.0102 g, 0.0168 mmol) and [Ph<sub>3</sub>C][B(C<sub>6</sub>F<sub>5</sub>)<sub>4</sub>] (0.0162 g, 0.0176 mmol), each in C<sub>6</sub>D<sub>5</sub>Br (0.5 mL), were prepared and cooled to  $-30^\circ\text{C}$ . The solutions were mixed while still cold, and the resulting orange solution was transferred to an NMR tube.

**{[MesNpy]<sub>2</sub>Hf<sub>2</sub>Me<sub>3</sub>}[B(C<sub>6</sub>F<sub>5</sub>)<sub>4</sub>].** Solutions of [MesNpy]HfMe<sub>2</sub> (0.318 g, 0.523 mmol) in C<sub>6</sub>H<sub>5</sub>Cl (1.5 mL) and B(C<sub>6</sub>F<sub>5</sub>)<sub>4</sub> (0.139 g, 0.271 mmol) in toluene (1.5 mL) were prepared and cooled to  $-30^\circ\text{C}$ . The solutions were mixed while still cold, and the resulting clear, colorless solution was stirred at room temperature for 15 min. The solvent was removed in vacuo and the remaining white residue triturated with pentane for 2 h and dried in vacuo; yield 0.628 g (69%). {[TripNpy]<sub>2</sub>Hf<sub>2</sub>(<sup>13</sup>Me<sub>3</sub>)[B(C<sub>6</sub>F<sub>5</sub>)<sub>4</sub>] was prepared in a similar fashion from [TripNpy]Hf(<sup>13</sup>Me)<sub>2</sub>. <sup>1</sup>H NMR (500 MHz, C<sub>6</sub>D<sub>5</sub>Br, 295 K):  $\delta$  1.00 (s, 4.5H, Zr-CH<sub>3</sub>), 1.17 (s, 3H, B-CH<sub>3</sub>), 1.18 (s, 3H, CH<sub>3</sub>), 1.23 (s, 6H, *o*-CH<sub>3</sub>), 2.17 (s, 6H, *o*-CH<sub>3</sub>), 2.31 (s, 6H, *p*-CH<sub>3</sub>), 2.90 (d, 2H, CH<sub>2</sub>), 3.86 (d, 2H, CH<sub>2</sub>), 6.72 (s, 2H, CH), 6.81 (s, 2H, CH), 6.92 (m, 1H, py-CH), 7.31 (m, 1H, py-CH), 7.52 (m, 1H, py-CH), 7.89 (m, 1H, py-*o*-CH). <sup>13</sup>C{<sup>1</sup>H} NMR (125 MHz, C<sub>6</sub>D<sub>5</sub>-Br, 233 K):  $\delta$  11.12 (br s, B-<sup>13</sup>CH<sub>3</sub>), 32.52 (s, Hf-<sup>13</sup>CH<sub>3</sub>), 41.35 (s, Hf-<sup>13</sup>CH<sub>3</sub>). Anal. Calcd for C<sub>76</sub>H<sub>78</sub>N<sub>6</sub>Hf<sub>2</sub>BF<sub>15</sub>: C, 52.82; H, 4.55; N, 4.86. Found: C, 52.67; H, 4.62; N, 4.73.

**Acknowledgment.** This research was supported in part by the Department of Energy (DE-FG02-86ER13564) and the U.S. Army through the Institute for Soldier Nanotechnologies, under Contract DAAD-19-02-D-0002 with the U.S. Army Research Office. The content does not necessarily reflect the position of the Government, and no official endorsement should be inferred. We also thank NSERC of Canada for a postgraduate scholarship (PGS B) to P.M.

OM030438I